Chapter 5
Molecular Imaging of Vascular Inflammation, Atherosclerosis, and Thrombosis

Dan Jane-Wit and Mehran M. Sadeghi

Introduction

Traditional Cardiovascular Imaging

Pathological changes in coronary artery anatomy are commonly used to guide management of patients with coronary artery disease (CAD) and other vascular diseases. To this end, anatomical imaging platforms like invasive angiography, contrast-enhanced computed tomography (CT) angiography, or magnetic resonance angiography (MRA) provide images of the vascular tree, allowing visualization of individual arteries. These techniques rely on detection of luminal stenosis (or dilatation). The severity of each lesion is estimated on the basis of anatomic size of the lumen compared to nondiseased artery segments. This information is used to guide therapy which may consist of medical management or invasive percutaneous or surgical revascularization. Despite providing highly informative data regarding arterial anatomy, angiography yields little information about the cellular constituents or tissue characteristics of the vessel wall. The presence of calcification is a notable exception which may be detected by invasive angiography or CT and provides information on the extent of atherosclerosis and potentially the likelihood of complications. High resolution anatomical images of

D. Jane-Wit, MD, PhD
Section of Cardiovascular Medicine, Yale University School of Medicine
and VA Connecticut Healthcare System, New Haven, CT, USA

Department of Immunobiology, Yale University School of Medicine,
New Haven, CT, USA

M.M. Sadeghi, MD (✉)
Section of Cardiovascular Medicine, Yale University School of Medicine
and VA Connecticut Healthcare System, West Haven, CT 06516, USA
e-mail: mehran.sadeghi@yale.edu

J.W. Homeister and M.S. Willis (eds.), *Molecular and Translational Vascular Medicine*,
Molecular and Translational Medicine, DOI 10.1007/978-1-61779-906-8_5,

the vessel wall may be obtained using intravascular ultrasound (IVUS) and more recently optical coherence tomography (OCT). Both techniques are invasive, i.e., require catheterization of arteries through small surgical procedures. Using IVUS, the "total vessel" and luminal areas as well as intimal thickness may be readily measured and aspects of vessel wall structure, including lipid core and calcification, may be identified [1]. OCT provides very high resolution (~10 μm) images of the vessel wall and can be used to define other aspects of atherosclerotic plaque structure, including the thickness of fibrous cap which is an important determinant of plaque stability. A major shortcoming of OCT is that its depth of imaging is limited to 1–2 mm [2].

Myocardial perfusion imaging (MPI) with platforms such as single photon emission computed tomography (SPECT), positron emission tomography (PET), magnetic resonance imaging (MRI), CT, or echocardiography assesses myocardial blood flow and defines the functional significance of coronary artery stenosis. Through detection of relative or absolute reduction in myocardial perfusion, ischemic territories (or those at risk for ischemia) can be qualified in terms of overall size, distribution, and severity. The size and severity of territories at risk for ischemia are functional indices that, similar to coronary anatomy, may be used to guide therapy. Importantly, the prognostic information on CAD obtained through physiological imaging with nuclear-based MPI is additive to the data provided by coronary angiography. Despite its strengths, MPI yields scant information regarding subcritical coronary stenoses or normal-appearing segments of the artery. Further, the stability of established atherosclerotic lesions cannot be assessed using functional indices provided in perfusion studies; hemodynamically significant but stable coronary lesions cannot be segregated from those which are imminently prone to rupture.

Molecular Imaging

By providing anatomic and functional data, traditional imaging provides valuable diagnostic and prognostic information, often in the setting of established and symptomatic vascular disease. Traditional imaging approaches are routinely used in clinical cardiovascular medicine (and basic research) and have contributed to the decline in cardiovascular mortality observed in recent decades. However, it is now well recognized that beyond the presence of flow-limiting stenosis, other aspects of vessel wall biology (e.g., vessel wall inflammation and matrix remodeling) are key determinants of propensity to vascular complications. Molecular imaging is an emerging field developed to address such limitations of traditional imaging. It refers to imaging techniques used to monitor and detect the spatial and temporal distribution of molecular or cellular processes in vivo [3]. Characterization, visualization, and quantification of the target process are inherent components of molecular imaging. Unlike traditional imaging which may rely on contrast agents with nonspecific (vascular or otherwise) distribution, in molecular imaging a

systemically administered probe specifically localizes to an area with a biologically relevant molecular or cellular process. The probe signal may be detected using one of the existing imaging modalities (platforms), including PET, SPECT, MRI, ultrasound, CT, or optical imaging. As described above, aberrancies in anatomy and physiology detected by classical anatomical and functional imaging are often late (and rather incomplete) manifestations of cardiovascular diseases. This limits the diagnostic and prognostic value of traditional imaging and restricts its use for biological studies. Molecular imaging can potentially overcome these constraints, thereby broadening the applications of noninvasive (or invasive) imaging studies. For example, rather than imaging the late consequences of atherosclerosis, various molecular and cellular events involved in the initiation and progression of atherosclerosis and development of its complications may be detected using specific probes. In aortic aneurysm, molecular imaging may identify small aneurysms at high risk for rupture. In cardiac transplantation, where late detection of graft arteriosclerosis is a major challenge to patient management, molecular imaging may identify the disease at an early stage where preventive and therapeutic approaches may be more effective. As such, widespread adoption of molecular imaging could lead to a paradigm shift in the management of many cardiovascular diseases. Molecular imaging may also serve as a powerful investigational tool for basic biological studies of cardiovascular diseases. Finally, by tracking the effect of therapeutic interventions in vivo, molecular imaging may facilitate cardiovascular drug development.

Challenges in Vascular Molecular Imaging

Molecular imaging is based on the premise that systemically administered probes (in trace amounts without detectable biological activity) can be selectively targeted to regions of interest to produce a specific signal strong enough for detection using an imaging platform. The abundance and accessibility of the target, properties of the ligand, and inherent capabilities of the imaging platform are key determinants of the feasibility and success of molecular imaging. In general, molecular imaging probes consist of conjugated ligands or substrates with high affinity, specificity, and selectivity for the target. The target should be abundant enough to generate a detectable signal. This is especially a challenge in vascular molecular imaging where the size of the target organ is a major limiting factor. Nevertheless, as described in the following sections, adhesion molecules, proteases, and scavenger receptors are examples of the classes of molecules which are highly induced in vascular pathology and have been successfully targeted for molecular imaging. A variety of ligands, including antibodies, peptides, and small molecules, have been used as the targeting moiety to generate highly specific and selective probes. Amplification of the signal has been achieved through a number of strategies, including intracellular sequestration of probe and the use of multivalent probes.

Enhanced endothelial cell permeability, such as that found in atherosclerosis, promotes access to subendothelial structures, and also can lead to nonspecific uptake of the probe which is a confounding factor in many imaging studies of the vessel wall biology. Due to close proximity of the vessel wall with circulating blood, the residual blood pool activity can mask a specific signal from adjacent structures. Alternatively, this can lead to false positive results secondary to changes in blood volume, for example, in the case of arterial aneurysm. These confounding factors underscore the importance of appropriate controls and careful analysis of the data in evaluating novel tracers for imaging vessel wall biology. Favorable probe pharmacokinetics are instrumental in vascular molecular imaging as high target-to-background ratios can only be achieved with relatively durable high-affinity binding to target molecules in concert with rapid clearance of nonbinding probes. Finally, cardiac motion is a hitherto unresolved major problem which has limited the application of molecular imaging to coronary pathologies. As shown in the following sections, this myriad of challenges has been met with varying degrees of success by investigators. Advances in technology and ongoing basic research combined with considerable clinical and pharmaceutical interest should facilitate the resolution of these challenges and ensure clinical translation of molecular imaging.

Molecular Imaging Platforms

In addition to their application in traditional anatomic and physiologic imaging, a growing number of imaging platforms are used for molecular imaging of the cardiovascular system. The strengths and limitations of each modality are reviewed in this section. A good understanding of these issues helps investigators and clinicians in selecting the most appropriate modality (or their combination) for each specific application.

Nuclear Imaging

Single Photon Emission Computed Tomography

Nuclear imaging techniques including SPECT and PET (discussed below) have functioned as the mainstay imaging platforms for molecular imaging for several decades. Both techniques use trace concentrations of radiolabeled probes (pM to nM) to provide a detectable signal. Similar to planar imaging, SPECT cameras detect the γ-rays emitted by radioisotopes such as ^{111}In, ^{123}I, and ^{99m}Tc. In SPECT imaging, true volumetric three-dimensional images are obtained which can be cross-sectioned in any direction. Because each radioisotope has a distinct energy profile, multiple tracers may be imaged simultaneously. This is especially important for imaging highly complex processes such as arthrosclerosis where a single tracer may not provide a full picture of the underlying biology. Compared to

other modalities discussed below, SPECT and PET are highly sensitive and widely available. A disadvantage of SPECT imaging is spatial resolution which is ~1 cm for traditional clinical cameras. For small animal imaging, microSPECT cameras equipped with pinhole collimators offer a resolution of ~1 mm for ^{99m}Tc [4, 5]. Like PET, SPECT exposes subjects to ionizing radiation.

Positron Emission Tomography

PET cameras detect high energy γ-rays generated after annihilation of positrons emitted by certain radioisotopes [6]. Clinical PET cameras intrinsically offer higher spatial resolution (4–5 mm) than SPECT cameras. However, for small animal imaging the free path of positrons before decay (~2 mm for ^{18}F) adversely affects microPET resolution relative to microSPECT imaging. Compared to SPECT, PET is an even more sensitive technique. In part, because of its high count statistics and good temporal resolution, PET imaging can provide absolute quantification of biological activity expressed as units of radioactivity per unit of volume. Unlike classical SPECT, PET may be used for dynamic imaging to delineate regional tracer flow or kinetics [7]. A disadvantage of PET imaging is the short half-life of PET radioisotopes (e.g., 2 h for ^{18}F), which necessitates close proximity to a cyclotron to generate imaging probes. The availability of positron emitting isotopes such as ^{11}C which may be incorporated into a probe without altering its physical and chemical properties is a major advantage of PET imaging.

Magnetic Resonance Imaging

In MRI an external magnetic field is applied to a subject, eliciting alignment with the magnetic field of certain nuclei (e.g., hydrogen) which normally spin in different directions. This alignment may be perturbed with a weak rotating radiofrequency pulse. The recovery of magnetization (relaxation) can subsequently be measured in either a plane parallel or longitudinal to the external magnetic field (T_1 relaxation time), or in a transverse plane (T_2 relaxation time). Inherent differences in relaxation times are exploited to generate contrast between different tissues. In the presence of contrast agents, e.g., gadolinium and iron oxide particles, the magnetic properties of the environment are altered, and a signal (whether positive or negative) is generated.

A major advantage of MRI compared to nuclear imaging is its high spatial resolution (25–100 μm) [8], which in combination with its excellent soft tissue contrast allows for combined anatomic and biologic imaging in one setting. This is especially important for imaging atherosclerosis where a combination of anatomical and biological features determine plaque vulnerability. The main limitation of MRI is low sensitivity [8]. As such, targeted imaging of the vessel wall often requires large micromolar concentrations of contrast agents which may potentially lead to untoward biological effects. Technical advances in probe development and alternative

imaging sequences (such as ^{19}F MRI) can potentially increase sensitivity, reduce background signal, and improve quantification capabilities of MRI [9].

Several probe platforms have been used for molecular MRI. Gadolinium shortens water proton T_1 relaxation times and generates a positive signal enhancement (white) on T_1-weighted images. Nanoparticle liposomes [10], lipid-encapsulated perfluorocarbon emulsions [11], and micelles [12] containing gadolinium chelates have been designed and tested in vivo for imaging of angiogenesis, thrombus, and atherosclerosis. Superparamagnetic iron oxide-based agents may be classified into different categories based on the diameter of the iron oxide core [13]. Iron oxide agents alter T_2 relaxation times, creating hypointense areas that appear black on T_2-weighted images. The negative enhancing signal associated with iron oxide uptake may be difficult to discriminate from negative enhancement associated with motion or flow artifacts. Signal loss is also heavily dependent on image resolution and regional contrast agent concentration. To overcome these limitations, several groups have developed "positive" MRI sequences (which generate white, hyperintense signals) to specifically detect sites of iron oxide uptake [14].

Ultrasound Imaging

Ultrasound imaging is based on the use of gas-filled microbubbles which resonate when exposed to ultrasound. The microbubbles are injected systemically and upon exposure to ultrasound waves become acoustically active, resonating at a frequency that can be detected using high-frequency sonographic probes. Selective accumulation of targeted microbubbles subsequently generates a bright (echogenic) signal at given regions of interest. Using antibodies and other ligands, these microbubbles are engineered to selectively bind to their targets [15]. A major advantage of ultrasound imaging is real time, inexpensive, and noninvasive imaging with relatively high spatial and temporal resolution. This facilitates serial imaging to monitor biological processes in vivo. The ability of ultrasound imaging to delineate anatomy further facilitates image acquisition and interpretation. A main limitation of ultrasound-based imaging is that the size of microbubbles limits its use in molecular imaging to endothelial or intravascular targets. Furthermore, high ultrasound frequencies required for high resolution vascular imaging are not optimal for microbubble detection [15].

Optical Imaging

Optical imaging, with its multitude of forms, is a highly versatile imaging modality that can be readily adapted for molecular imaging applications [16, 17]. The most common optical imaging technique for cardiovascular molecular imaging is fluorescence. Fluorescent imaging relies on fluorescent probes that upon excitation with external light emit light at higher wavelengths. These probes may fit into one of three categories: nontargeted (e.g., indocyanine green for angiography), targeted

(ligands conjugated with fluorochromes), or activatable. The fluorescence in an activatable probe is in a quenched state at baseline, and can be dequenched upon cleavage of a specific substrate by an enzyme. This approach is associated with less background than other categories of probes and can provide highly sensitive information about enzymatic activity [18]. Distinct excitation and emission spectra of different fluorophores allow for simultaneous imaging of multiple targets in vivo. Given the exquisite sensitivity of optical imaging, fluorescent probes may be used at low concentrations and detect targets in the picomolar range. Besides versatility and sensitivity, a major strength of fluorescent imaging is spatial resolution which, depending on the detection system, can be in the μm to mm range. Limitations of in vivo fluorescent imaging include tissue autofluorescence, light scatter (refraction of signal traversing through body tissue), and depth of penetration (millimeter to low centimeter range). In addition, the chemical environment in tissue may affect fluorescence, contributing to inaccuracies and difficulties in quantification of the fluorescent probe concentration in deep tissues. Some of these limitations are in part overcome with imaging in the near infrared (NIR) window (excitation between the wavelengths of 650–900 nm). NIR fluorescent imaging is associated with reduced autofluorescence and markedly less photon absorption by hemoglobin and other endogenous molecules. As such, deeper tissues may be imaged. A new imaging platform, fluorescence molecular tomography (FMT), aims at producing mathematically derived three-dimensional images and quantitative information on fluorescent probe concentration in deep tissues [18, 19].

Computed Tomography

Differential attenuation of X-rays by various tissues is the basis for CT imaging which is classically performed for high contrast-high resolution anatomical imaging. This, in combination with newer techniques, including multislice and dual energy imaging, can provide information on the extent of atherosclerosis, presence of calcified or low attenuation plaques, and remodeling in coronary arteries. As such, while not molecular imaging in its purest definition, CT imaging may identify aspects of plaque biology that determine its propensity for complications. Hybrid imaging with CT (PET/CT, SPECT/CT) is used for signal localization, attenuation correction, and partial volume correction for molecular nuclear imaging. A recent application of CT involves contrast containing nanoparticles for detection of macrophage phagocytic activity in atherosclerosis [20].

Vascular Biology Processes as Targets for Molecular Imaging

Vascular diseases share a set of critical overlapping basic biological processes. These processes, whether alone or in combination, may serve as targets for molecular imaging, and their imaging can provide important and often unique information on the initiation, progression, and response to therapy of vascular diseases.

Endothelial cell activation, inflammation, angiogenesis, matrix remodeling, apoptosis, and thrombosis are especially important in the pathogenesis of atherosclerosis. In parallel with advances in technology, considerable progress has been made in recent years in imaging these processes, and some of the approaches initially validated in animal models are at the cusp of entering clinical practice. The following section, albeit by no means exhaustive, reviews some of the key recent developments in molecular imaging of atherosclerosis, inflammation, and thrombosis with a focus on vascular imaging.

Inflammation is critical to initiation, progression, and instability of the atherosclerotic plaque [21]. Retention of low-density lipoprotein (LDL) in the vessel wall and endothelial cell activation promote the recruitment, activation, and accumulation of inflammatory cells in early atherosclerotic lesions. Lipid phagocytosis by monocyte-derived macrophages, release of free radicals, and the resultant generation of modified lipids in conjunction with local production of chemokines and cytokines sustain a proinflammatory milieu, which further promotes the development of atherosclerosis. Through outward remodeling, the lumen area remains preserved in even fairly advanced atherosclerotic lesions. However, with the progression of plaque, the lumen eventually narrows down to the degree that the lesion may become symptomatic. Symptoms of ischemia may also occur when plaques rupture or erode which then exposes blood to the procoagulant subendothelial structures, promoting focal thrombus formation and sudden reduction in blood flow [22–24]. Plaque rupture (and healing) also contributes to rapid increases in plaque size. The mechanisms of plaque erosion are poorly understood. However, it is now well established that plaque rupture is linked with the presence of high densities of inflammatory cells that through production and activation of various proteases weaken a thin fibrous cap. In addition to its key role in atherosclerotic plaque progression and rupture, vessel wall inflammation plays an important role in other vascular diseases. Aortic aneurysm and transplant vasculopathy are examples of other vascular diseases where the presence of inflammatory cells (including macrophages, T lymphocytes, and dendritic cells) is linked with pathogenesis of the disease and its complications.

While the presence of edema and certain patterns of light scatter (in the case of OCT [2]) may detect aspects of inflammation, targeted molecular imaging stands out as a uniquely powerful tool for imaging vessel wall inflammation. Endothelial cell activation, inflammatory cell recruitment, activation and death, protease activation, vascular smooth muscle cell (VSMC) proliferation, and angiogenesis are intertwined processes that contribute to or are the result of vessel wall inflammation. To facilitate the discussion, approaches to imaging each process are reviewed under a separate heading.

Endothelial Activation

The endothelium serves as an active barrier between blood and subendothelial cell structures. In response to injury or proinflammatory cytokines, endothelial cells

convert to a procoagulant, proadhesive phenotype and this barrier is disrupted. The disruption of endothelial cell barrier function may be detected based on passive diffusion of labeled macromolecules [e.g., ^{99m}Tc-polyclonal immunoglobulin (~150 kDa), Gd-DTPA-albumin (~70 kDa)] [25]. In atherosclerosis imaging, this passive diffusion promotes the delivery of both targeted and nonspecific probes beyond the endothelium.

Endothelial activation is an early step in the initiation of atherosclerosis. Vascular cell adhesion molecule-1 (VCAM-1) is inducibly expressed on the adluminal surface of activated endothelial cells during the acute, early stages of vascular inflammation [26]. Upregulation of VCAM-1 mediates leukocyte adhesion and their subsequent transmigration through the vessel wall. In addition to endothelial cells covering the lumen of arteries prone to atherosclerosis, a large number of endothelial cells are present within the neovessels (vasa vasorum) of atherosclerotic plaque and its vicinity. As such, selective expression of VCAM-1 on activated and dysfunctional endothelial cells has rendered VCAM-1 a natural candidate for visualization of inflammation associated with atherogenesis [27].

Several probes have been developed for targeted visualization of VCAM-1 expression using MRI or optical imaging [28, 29]. In one approach, microparticles of iron oxide (MPIO) which contain large amounts iron oxide were decorated with an anti-VCAM-1 antibody and selectively localized to sites of IL-1β-induced cerebral vascular inflammation in murine hosts. These sites could be conspicuously visualized noninvasively with MRI [28]. In another approach, peptide sequences with homology to $\alpha_4 \beta_1$ integrin, a native ligand for VCAM-1, were selected through phage display screening [30, 31]. These were incorporated into multivalent nanoparticles to generate probes detectable by MRI and optical imaging. One such probe, VINP-28, localized to aortic root atherosclerotic lesions in murine hosts and was able to discriminate response to statin therapy by MRI [31]. More recently, a VCAM-1-specific tetramer peptide labeled with ^{18}F was used to assess atherosclerosis and response to therapy in apoE$^{-/-}$ mice by PET [32]. Of note, these peptides have been selected against murine VCAM-1 and their binding to human VCAM-1 has not been demonstrated. In addition, a previous report has questioned whether there are sufficient numbers of VCAM-1 molecules for imaging on human endothelial cells [27].

Endothelial cell adhesion molecules are ideal targets for ligand-coated microbubbles, which can be detected by ultrasound imaging. As such, intercellular adhesion molecule-1 (ICAM-1) targeted microbubbles were shown to bind to activated endothelial cells [33]. Microbubbles coated with antibodies against VCAM-1, P-selectin, or their combination have been successfully used to detect endothelial activation in murine models of atherosclerosis (Fig. 5.1) [34, 35]. Other probes targeting adhesion molecules such as E-selectin, P-selectin, or ICAM-1 [36–38] have similarly been investigated as noninvasive means to detect acute cerebrovascular inflammation by MRI.

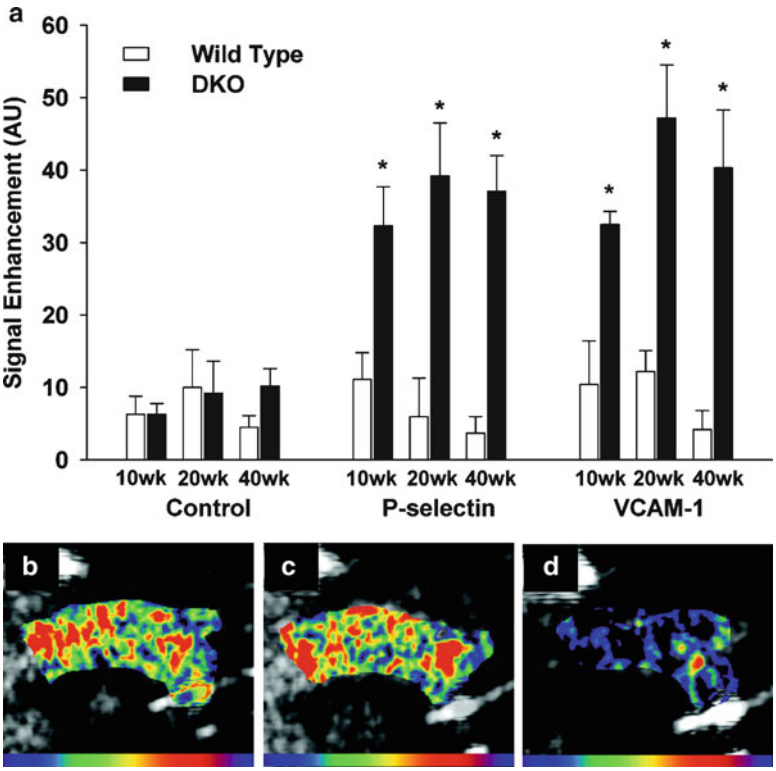

Fig. 5.1 Contrast-enhanced ultrasound images of aortic arch using VCAM-1-targeted (**a** and **b**), P-selectin-targeted (**a** and **c**) or control (**a** and **d**) microbubbles in wild-type (WT) or LDL receptor and apobec-1 double knock out (DKO) mice at 10, 20, or 40 weeks of age. (**a**) Background-corrected signal intensity in the proximal aorta, $^{*}p < 0.05$. (**b**–**d**) Examples of targeted ultrasound imaging in 40-week-old double knockout mice, demonstrating the presence of a high signal (in *red* and *yellow*) in the aortic arch with VCAM-1- (**b**) and P-selectin (**c**)-targeted probes. Reprinted from [35] with permission from Lippincott Williams & Wilkins

Lipid Accumulation

LDL and its modified derivatives play an important role in the initiation and progression of atherosclerosis, and plaque vulnerability has been linked with the presence of a large lipid-laden necrotic core [39, 40]. IVUS is an invasive tool used for assessing lipid core which appears as an area of echolucency on IVUS and its size has been linked with clinical events [41, 42]. However, echolucency is not specific for lipid core and may also be seen with intraplaque hemorrhage. MRI can characterize plaque components, including its lipid content with accuracy [39, 43]. More recently, CT angiography has been proposed for assessing plaque volume (in part related to the size of necrotic core) with relative accuracy [44].

Molecular imaging can complement these data by providing important additional information, including the presence of lipid modification and specific receptors in atherosclerosis. Radiolabeled LDL (e.g., with ^{125}I, or ^{99m}Tc) was one of the first agents used for plaque characterization in animal models of arthrosclerosis [45–47]. Due to slow clearance of the labeled probes, this approach was found to be ineffective for in vivo imaging and was abandoned. Other early approaches to imaging lipids in atherosclerosis included the use of labeled lipoprotein derivatives and oxidized LDL [48, 49]. Eventually, all these were abandoned for a targeted approach aimed at detecting lipid modification and receptors involved in lipid uptake in atherosclerosis. MDA2, an antibody raised against a neoepitope found on oxidized LDL, and other similar antibodies have been incorporated into various imaging probes. Labeled MDA2 localizes in atherosclerotic lesions in murine and rabbit models of atherosclerosis, and its imaging can track the effect of dietary intervention on plaque development [50–52]. Interestingly, in rabbit atherosclerosis, macrophage immunostaining is prominent in plaque areas with high MDA2 uptake, while areas with less uptake show stronger staining for collagen and VSMCs [52]. Targeted micelles incorporating MDA2 and other similar antibodies localize within macrophages of atherosclerotic plaques in apoE$^{-/-}$ mice [53, 54]. It is reported that membranes of cells undergoing apoptosis express higher levels of oxidized phospholipids, which may be targeted by oxidation-specific antibodies [55]. As such, micelles incorporating these antibodies may be used for in vivo assessment of complementary aspects of plaque biology by MRI.

Macrophage Biology

Radiolabeled leukocytes are traditionally used to identify sites of inflammation by nuclear imaging in humans. A similar approach was used to assess monocyte trafficking to atherosclerotic lesions by autoradiography and microSPECT imaging [56, 57]. Purified syngeneic monocytes labeled with ^{111}In-oxine were injected to apoE$^{-/-}$ mice and were detected in atherosclerotic lesions within 5 days after intravenous administration. Monocyte accumulation in the vessel wall increased with age of the mice and correlated with plaque area in animals of different ages and on different diets [56]. Importantly, microSPECT imaging demonstrated an approximately fivefold reduction in monocyte trafficking in animals treated with various statins [57]. Radiolabeling of leukocytes is clearly a powerful experimental tool for quantifying the trafficking of leukocyte subpopulations in atherosclerosis. However, changes in focal leukocyte numbers due to cell proliferation or apoptosis cannot be differentiated by this approach.

Activated macrophages display surface proteins that confer sensitivity to chemokines. One such surface protein, CCR-2, the receptor for macrophage chemotactic protein-1 (MCP-1), was exploited as a target to noninvasively visualize macrophages in atherosclerotic plaques. In a rabbit model of atherosclerosis, ^{99m}Tc labeled MCP-1 uptake (presumably by macrophages) in the balloon-injured

aorta could be visualized using SPECT imaging. Furthermore, tracer uptake quantified ex vivo correlated well with macrophage immunostaining in atherosclerotic lesions [58].

Exploiting the phagocytic phenotype of activated macrophages, investigators have used iron oxide particles as a selective probe for imaging macrophages using MRI [59]. Microcrystalline iron oxide particles coated with dextrans or siloxanes can be efficiently delivered to resident macrophages in atherosclerotic plaques at sufficient density as to generate negative MRI contrast on T_2- or T_2^*-weighted images. Initially tested in rabbit models of atherosclerosis [60, 61], the observation on negative plaque enhancement using superparamagnetic iron oxide particles has been extended to humans [62–64]. Importantly, in a study in symptomatic human carotid disease, ultrasmall particles of iron oxide (USPIO) accumulation in carotid arteries was detectable by MRI as early as 24 h and colocalized with areas of high macrophage content on endarterectomy samples [64]. The exact mechanism of ultrasmall particles of iron oxide uptake in plaque macrophages is not clear, and may involve transmigration of monocytes that have endocytosed the particles in the blood, or diffusion of ultrasmall particles of iron oxide into subendothelial space due to enhanced vascular permeability and their subsequent in situ uptake [59]. A number of confounding factors should be considered when using iron oxide particles for imaging macrophages in atherosclerosis. Superparamagnetic iron oxide uptake is not specific to macrophages or reticuloendothelial cells and can be seen by other cell types [59]. The size of the particles, their coating and charge and the cell type determine the mechanisms through which the particles are taken up by target cells. The extent of signal drop and concentration of iron oxide particles in the vessel wall may not be linear under every experimental condition. Finally, there are major differences in iron particle clearance between different species which should be considered in extrapolating observations made in rodents to humans [59]. The development of multimodal magnetofluorescent nanoparticles (MFNPs) provided an opportunity to directly investigate the localization of iron oxide particles. When injected to atherosclerotic apoE$^{-/-}$ mice, plaque macrophages represented ~65% of MFNP-positive cells with the rest consisting mostly of endothelial and VSMCs [65]. Similarly, a ^{64}Cu-labeled multimodal nanoparticle has been developed and validated for in vivo imaging of inflammation in murine atherosclerosis [66]. More recently, an iodinated nanoparticle contrast agent that is phagocytosed and accumulates in macrophages, N1177, has been developed and tested for CT imaging of atherosclerosis in rabbits [20]. CT enhancement using this agent correlates well with ^{18}F-FDG uptake and macrophage immunostaining [67]. It remains to be determined whether this enhancement is of sufficient magnitude for imaging human atherosclerosis.

Scavenger receptors are pattern recognition receptors that were initially identified based on their ability to mediate cellular uptake of modified (e.g., by oxidation or acetylation) LDL. They now include a diverse group of proteins categorized into eight classes based on their structural homology [68]. Over the years it has become clear that in addition to modified LDL, these receptors bind to many other ligands. Macrophages express several scavenger receptors, including scavenger receptor A (SR-A), CD36, CD68, and lectin-like oxidized LDL receptor 1 (LOX-1) [69].

Scavenger receptor AI (SR-AI), one of the first modified LDL receptors identified, is upregulated in the course of macrophage differentiation [70]. Based on this observation and low levels of SR-A expression in normal arteries, gadolinium-containing SR-A targeting immunomicelles were used for detecting macrophages in aortic wall of apoE$^{-/-}$ mice by MRI [12]. Consistent with SR-A expression pattern, much (but not all) of the immunomicelle uptake colocalized with CD68 positive areas and there was a strong correlation between gadolinium signal enhancement and CD68 staining.

LOX-1 is an inducible scavenger receptor that was originally discovered in endothelial cells [71, 72], but is also expressed on the surface of macrophages and VSMCs [73]. Using a ^{99m}Tc-labeled anti-LOX-1 antibody, atherosclerotic aortas could be visualized in Watanabe heritable hyperlipidemic rabbits by planar imaging [74]. In Watanabe heritable hyperlipidemic rabbit aortas, ^{99m}Tc-labeled anti-LOX-1 antibody uptake was twofold higher than the uptake of a control antibody. The difference was tenfold between ^{99m}Tc-labeled anti-LOX-1 antibody uptake in the aortas of Watanabe heritable hyperlipidemic compared to control rabbits, underscoring the magnitude of nonspecific tracer uptake in atherosclerosis. Tracer uptake in atherosclerosis correlated well with a vulnerability index defined as the ratio of lipid component area (macrophages and extracellular lipid deposits) to the fibromuscular component area (smooth muscle cells and collagen fibers) [74]. Similarly, a second probe targeted against LOX-1 has been validated for detection of atherosclerotic lesions in vivo [75]. This probe was designed for use across multiple imaging platforms and consists of a liposomal shell coated with anti-LOX-1 antibody, Dil (1,1-dioctadecyl-3,3,3′,3′-tetramethylindocarbocyanine perchlorate) fluorescent molecules and either gadolinium or ^{111}In. In vivo, this probe was shown to preferentially bind to macrophages and localize in the shoulder region of plaques.

Enhanced cellular metabolic activity mainly attributed to macrophages in atherosclerosis may be detected by ^{18}F-2-deoxy-D-glucose (FDG) PET imaging [76]. Cellular uptake of ^{18}F-FDG, a glucose analog, is mediated by glucose transporters. Once inside the cell ^{18}F-FDG is phosphorylated by hexokinase to ^{18}F-FDG-6-phosphate which cannot be further metabolized and is trapped inside the cell. Retained ^{18}FDG can be detected by PET imaging and ^{18}F-FDG-6-phosphate eventually decays to glucose-6-phosphate. ^{18}F-FDG uptake is seen in several leukocyte populations, including human monocyte-derived macrophages in culture, where uptake level is comparable to several cancer cell lines [77]. Hexokinase activity is considerably enhanced in activated macrophages [78] and macrophage activation leads to enhanced ^{18}F-FDG uptake [77]. Interestingly, ^{18}F-FDG uptake by human endothelial cells in culture is reported to be several folds higher than macrophages [79].

^{18}F-FDG uptake can be detected in rabbit atherosclerosis and the uptake correlates with macrophage density [80–82]. ^{18}F-FDG PET imaging following administration of Russell's viper venom to induce aortic thrombosis (presumably due to plaque rupture) in atherosclerotic rabbits showed slightly (albeit nonsignificantly) higher ^{18}F-FDG uptake in thrombosed areas [83]. Importantly, treatment with probucol (an antihyperlipidemic drug with antioxidant properties) led to a significant reduction in ^{18}F-FDG uptake in parallel with the reduction in macrophage infiltration

in WHHLMI rabbit aortas [84]. There are conflicting data on ^{18}F-FDG uptake in atherosclerotic mice, some of which may be related to the timing of imaging [85, 86]. It is reported that ^{18}F-FDG binds to sites of vessel wall calcification, presumably through nonspecific entrapment by hydroxyapatite [87].

Expression of integrins by inflammatory cells has raised the possibility that integrin imaging may be used to detect vascular inflammation. Arginine–glycine–aspartate (RGD)-based peptides bind to integrins with the flanking sequences determining selectivity for specific members of the integrin family. Integrin $\alpha_v\beta_3$ (discussed more in detail later in this section) is expressed at high level on monocytes and macrophages. ^{18}F-galacto-RGD, a probe targeting α_v integrins, localizes in areas rich in nuclei (presumably consisting mostly of macrophages) in murine aortic atherosclerosis [88]. Similarly, an optical probe RGD-Cy 5.5 was used to image lesions induced by carotid ligation in high fat-fed apoE$^{-/-}$ mice [89]. Histological analysis demonstrated colocalization of the tracer with macrophages in carotid lesions.

Matrix Remodeling

Extracellular matrix serves as an anchoring scaffold for cellular constituents of tissues. Matrix remodeling through synthesis, reorganization, and degradation of macromolecules plays a central role in the pathogenesis of vascular diseases. Matrix remodeling is an integral part of vascular remodeling, a process that involves persistent changes in vessel wall composition and geometry. The two components of vascular remodeling, geometrical remodeling, and changes in vessel wall composition play a more or less prominent role in specific vascular diseases. For example, in aortic aneurysm, expansive (outward) remodeling of the artery is most prominent, while in transplant vasculopathy, intimal hyperplasia may be considered the key pathological feature. In atherosclerosis both components of vascular remodeling play major and complementary roles in the development of an atherosclerotic plaque and its complications. Compared to those plaques with inward (negative, constrictive) remodeling, atherosclerotic plaques with outward (positive, expansive) remodeling have higher lipid and macrophage content, features that are associated with plaque vulnerability [90]. This association of remodeling with plaque composition (and propensity to rupture) has been repeatedly observed in other studies, including a study in patients with renal artery stenosis where the necrotic core was found to be larger in lesions with positive remodeling [91, 92].

In addition to its role in geometrical remodeling and intimal hyperplasia, matrix remodeling plays a direct role in plaque rupture. A recent prospective study in patients undergoing percutaneous coronary interventions for acute coronary syndromes (which excluded patients with any remaining lesion with diameter stenosis >50%) did not find any association between remodeling index (dichotomized around the median value of 0.94) and major adverse cardiovascular events (MACEs) over a 3-year follow-up period [1]. However, relevant to the discussion on matrix

remodeling, compared to plaques not associated with MACEs, those associated with MACEs were more likely to have been classified as thin-cap fibroatheromas (defined by radiofrequency-IVUS) in the initial analysis [1]. This is presumably because the thin-cap fibroatheromas are more prone to rupture. It is believed that reduced matrix protein synthesis secondary to VSMC paucity and enhanced matrix degradation due to high density of inflammatory cells weaken the fibrous cap and predispose it to rupture.

Matrix turnover is mediated by several families of proteases including adamalysins [93], matrix metalloproteinases (MMPs) [94], cathepsin cysteine proteases [95], and serine proteases [96]. Of these, MMPs and cathepsins have been used as targets for molecular vascular imaging. The MMP family consists of at least 23 secreted and membrane-bound zinc and calcium-dependent endopeptidases which may be classified into different classes based on their structure or preferred substrates [94, 97, 98]. Expression of collagenases (MMP-1, -8, -13), gelatinases (MMP-2, -9), stromelysins (MMP-3, -10, -11), matrilysins (MMP-7), and membrane-bound MMPs (MMP-14) and other MMPs (MMP-12) has been reported in atherosclerosis and related diseases [98]. Collectively, these proteins are potent proteases that catalyze the degradation of connective tissue and extracellular matrix components including fibrillar and nonfibrillar collagens, elastin, and basement membrane glycoproteins.

Matrix Metalloproteinases

In addition to their direct effect on matrix proteins, MMPs regulate vessel wall biology through other mechanisms, including proteolytic cleavage and release of cytokines, chemokines, and growth factors. ECs, VSMCs, and inflammatory cells are the main sources of MMP activity in the vessel wall [94, 98]. A large body of evidence exists on the role of MMPs in the pathogenesis of atherosclerosis, and its complications, as well as other vascular diseases [98]. As discussed above, MMPs modulate plaque stability through regulation of extracellular matrix protein deposition and degradation, and also VSMC proliferation, and inflammation [94, 99, 100]. Different members of the MMP family have distinct effects on plaque biology. As such, atherosclerosis in apoE/MMP-12 double knockout mice shows features associated with plaque stability, i.e., increased VSMC and reduced macrophage content compared to mice deficient in apoE alone [101]. Similarly, VSMC content, a feature of plaque stability, is increased in apoE/MMP-7 double knockout mice. This is in contrast to the effect of MMP-3 or MMP-9 deletion which confer features of plaque instability to atherosclerotic lesions [101].

MMP activity is regulated at transcriptional and posttranscriptional levels. With a few notable exceptions, MMPs are in general produced as inactive secreted or membrane-bound proenzymes. MMP activation involves delocalization of the so-called MMP prodomain through enzymatic cleavage or allosteric displacement to expose the zinc-dependent catalytic domain [97]. Substrate specificity is in part determined by binding to sites other than the catalytic site (so-called exosites) which

may serve as targets for tracer development in the future. Interaction with other molecules including *t*issue *i*nhibitors of *M*M*Ps* (TIMPS) and compartmentalization are additional mechanisms of regulating MMP activity [97].

Two strategies have been developed for imaging MMP expression and activity in vascular diseases. The first strategy exploits the enzymatic activity of MMPs. In one approach, following enzymatic cleavage of a specific substrate, quenching fluorochromes are removed from an optical probe, generating a fluorescent signal detectable by optical imaging [102]. In theory, this approach allows for high specificity based on the substrate structure, low background activity, and considerable signal amplification in the presence of MMP activity. One such probe that incorporates a peptide sequence recognized by MMP-2 and MMP-9 was used to detect MMP activity in murine atherosclerosis. Ex vivo images demonstrated localization of the probe in macrophage-rich areas of atherosclerotic aorta [103]. A similar probe that can be activated in vitro in the presence of MMP-13, MMP-12, MMP-9, MMP-7, MMP-2, and MMP-1 was used to detect MMP activation in aortic aneurysm in fibulin-4 mutant mice (a model of Marfan's disease) [104]. Interestingly, in this model, tracer uptake in the aorta preceded the development of aneurysm. An alternative approach based on enzymatic activity involves the use of activatable cell-penetrating peptides. In this approach, cleavage of the substrate allows a cell-penetrating peptide to enter the cells [105]. While promising, this approach has not been tested for imaging vascular pathologies, and a recent report suggested that rather than occurring in the vicinity of target cells, activation of the peptide occurs remotely in the vascular compartment, indicating that it might not be optimal for vascular imaging [106].

An alternative strategy for imaging MMPs employs ligands, including MMP inhibitors, which selectively bind to MMPs. Based on such ligands, several radiolabeled probes, including ^{123}I-CGS 27023A, ^{111}In-RP782, and ^{99m}Tc-RP805, have been developed and used to image MMP expression in the vessel wall. When administered intraorbitally, ^{123}I-HO-CGS 27023A localized in ligated carotid arteries in apoE$^{-/-}$ mice yielding a signal that was detected by planar imaging [107]. A subsequent study using ^{111}In-labeled RP782, a tracer that specifically binds to the activation epitope of multiple MMPs, demonstrated considerable uptake of the tracer in murine carotid arteries following wire injury [108]. In this model, carotid injury leads to considerable neointimal hyperplasia over a period of 4 weeks, which predominantly consists of VSMCs. Tracer uptake was detectable in vivo by microSPECT/CT imaging by 2 weeks (and by autoradiography, a more sensitive technique, as early as 1 week) after injury. Consistent with the role of MMPs in vascular remodeling, RP782 uptake paralleled weekly changes in the cross-sectional vessel wall, but not total vessel or luminal, area [108]. In a follow-up study, serial microSPECT/CT imaging at 2 and 4 weeks after carotid wire injury with RP805, a ^{99m}Tc-labeled homologue of RP782, was used to assess the effect of dietary intervention on vascular remodeling. Tracer uptake (reflecting MMP activation) in injured arteries was reduced as early as 1 week after withdrawal of a high fat diet. Furthermore, MMP activation in the vessel wall detected by noninvasive imaging at 2 weeks after injury correlated well with neointimal area at 4 weeks in the same

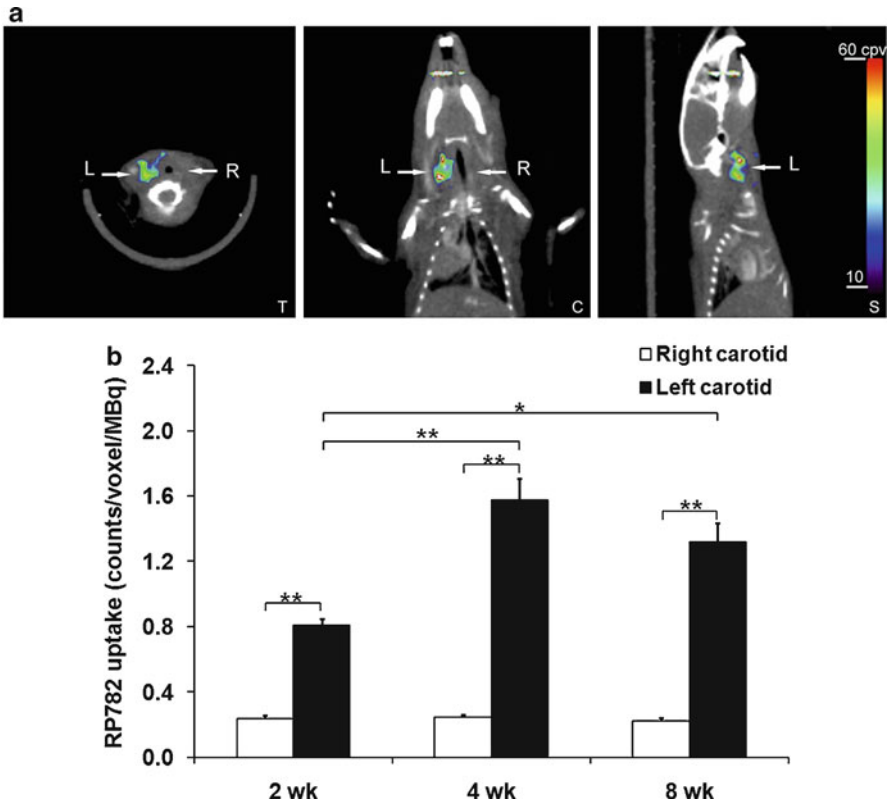

Fig. 5.2 MMP-targeted imaging of carotid aneurysm. (**a**) RP782 microSPECT/CT images of an apoE$^{-/-}$ mouse at 4 weeks after surgery to induce left common carotid artery aneurysm, demonstrating higher tracer uptake in aneurismal left (L) than control right (R) carotid artery. (**b**) Quantification of tracer uptake in carotid arteries at 2, 4, and 8 weeks (wk) after surgery. $^{*}P = 0.01$; $^{**}P < 0.001$. *C* coronal slice, *S* sagittal slice, *T* transverse slice. Reprinted by permission of the Society of Nuclear Medicine from [110]

animal, indicating that MMP-targeted imaging may be used to predict the effect of therapeutic interventions on intimal hyperplasia [109]. Similarly, in a model of $CaCl_2$-induced carotid aneurysm in apoE$^{-/-}$ mice, MMP-targeted imaging was able to predict the propensity of an aneurysm to expansion in vivo [110] (Fig. 5.2). Similar tracers were used to detect MMP activation in rabbit [111, 112] and murine [113] models of atherosclerosis. In rabbit atherosclerosis, MMP tracer uptake in atherosclerotic aortas was detectable by planar imaging [111]. Ex vivo quantification of tracer uptake in the aorta showed a significant reduction in MMP activation in animals treated with a statin, minocycline (an MMP inhibitor), or high fat withdrawal [112, 113]. There was a good correlation between tracer uptake and macrophage immunostaining. Similarly, a correlation existed between aortic macrophage immunostaining and ex vivo quantification of tracer uptake in the mouse models of atherosclerosis [113].

P947 is a novel MR contrast agent with μM affinities for various MMPs obtained by coupling gadolinium to an MMP inhibitor [114]. Ex vivo, this agent can bind to MMP-rich human carotid endarterectomy samples. When injected to atherosclerotic mice, considerable signal enhancement may be detected in the aorta by in vivo MRI [114]. Using a fluorescent homologue, it was shown that P947 localizes near the fibrous cap of murine atherosclerotic plaques in areas positive for MMP-2, MMP-3, and MMP-9 immunostaining [115]. A similar enhancement of the aortic wall was observed in rabbits fed a high fat diet. Repeated MRI after 4 months in animals that continued the high fat diet showed persistence of the signal. However, in animals switched to normal chow, in conjunction with the reduction in MMP-2 activity, the signal was significantly reduced on repeat MRI [116]. MRI in a rat model of abdominal aortic aneurysm showed significantly higher normalized signal enhancement with P947 compared with an inactive homologue or Gd-DOTA [117]. P947 signal enhancement was also higher in aneurismal, as compared to sham operated, aortas. The predictive value of this approach for aneurysm expansion remains to be determined.

Cathepsins

Cathepsins are a group of 11 predominantly intracellular enzymes that belong to the family of cysteine proteases [95]. They are produced as preproenzymes with enzyme activation occurring in endoplasmic reticulum, endosomes, or lysosomes. Enzyme activity is regulated by a group of inhibitors including cystatin C. It is reported that human macrophages secrete cathepsins B, L, and S into the peri-cellular space. Several cathepsins including cathepsins B, K, and S are expressed in human and murine atherosclerosis where cathepsin immunostaining localizes to macrophages, endothelial cells, and VSMCs. Cathepsins modulate atherosclerosis through regulation of elastase and collagenase activity, lipid metabolism, and inflammation [118]. Deletion of cathepsin S in atherosclerosis-prone mice leads to reduction of plaque area [119]. Cathepsin K deletion similarly leads to smaller plaques with reduced frequency of rupture in brachiocephalic artery [120].

An activatable near infrared fluorescent (NIRF) probe with poly-L-lysine backbone was initially developed for imaging cathepsin enzymatic activity in tumors [121] and has been used to detect proteolytic activity in atherosclerotic lesions in the mouse [122]. The activity of the probe was validated in the presence of tumor cells capable of internalizing the probe [121]. Protease inhibitors such as E64 (which inhibits cathepsins B, H, L and a number of other proteases) and leupeptin (a serine, cysteine, and threonine protease inhibitor) completely inhibited NIRF signal generation. A similar inhibitory effect was seen for trypsin inhibitor (tosyl-L-lysyl chloromethyl ketone) and trypsin-like serine protease inhibitor (3,4-dichloroisocoumarin), but not pepstatin, a cathepsin D inhibitor [121]. In apoE/eNOS double knockout mice on a Western-type diet, it was shown that cathepsin B is upregulated in atherosclerotic lesions and following administration of the probe, the resultant fluorescent signal can be detected in vivo by fluorescence-mediated tomography. On ex vivo analysis, fluorescent activity localized in the aortic arch

and abdominal aorta. Fluorescent activity on microscopy was detected in the endothelial and subendothelial areas which were also positive for cathepsin B immunostaining [122]. The same cathepsin B probe was used to assess protease activity ex vivo in human endarterectomy samples [123]. Protease-related fluorescent signal was present both in the plaque and in emboli obtained at the time of intervention, and subtle differences in signal distribution was observed between plaques from symptomatic and asymptomatic patients. An activatable MMP probe generated a similar signal which localized in the vicinity of macrophage-rich areas of the plaque [123]. Cathepsin K is expressed by macrophages and VSMCs and shows considerable elastinolytic and gelatinolytic activity. A probe, incorporating a cathepsin K sensitive peptide, was used for imaging proteolytic activity in mouse aortic atherosclerosis and in human carotid endarterectomy samples [124]. This probe demonstrates twofold higher sensitivity for cathepsin B compared to other cathepsins and a ~10-fold higher sensitivity compared to MMPs. In both models, considerable fluorescent signal was generated by the probe. Interestingly, while both VSMCs and macrophages express cathepsin B, the signal localized mostly with macrophages, but not VSMCs, indicating differences in cathepsin activation or secretion or probe uptake between the two cells [124]. Novel derivatives of protease sensors with different pharmacokinetics and sensitivity have been developed and evaluated for their binding to atherosclerotic lesions in the mouse [125]. To overcome depth-related limitations of optical imaging, a catheter-based strategy for detection of NIRF has been developed and tested in the aorta of atherosclerotic rabbits [126]. Some of the limitations and technical difficulties associated with endovascular NIRF imaging may be addressed using novel algorithms developed for quantitative imaging through blood [127].

Fibronectin

Imaging neoepitopes on matrix proteins is a complementary approach to detection of matrix remodeling. One such epitope is the extra-domain B (ED-B) of fibronectin which is generated by alternative splicing during angiogenesis and remodeling [128]. Radiolabeled and fluorescent-labeled antibody against ED-B localizes in atherosclerotic, but not normal artery and the corresponding signal can be detected ex vivo. In combination with imaging protease activation or activity, these molecular imaging approaches have become powerful experimental tools for assessing vascular remodeling in vivo, and their imminent clinical application may have a transformational effect on diagnostic and therapeutic approach to vascular diseases.

Smooth Muscle Proliferation

VSMCs play a dual role in atherosclerosis. On one hand, proliferation and migration of VSMCs into the developing plaque is an early step in atherogenesis [129].

Activated VSMCs produce inflammatory mediators and matrix proteins that promote plaque development and its stability. On the other hand, plaque rupture is linked with a paucity of VSMCs and the resultant thinning and weakening of the fibrous cap. In other diseases, e.g., in-stent restenosis and transplant vasculopathy, VSMC proliferation is predominantly a pathogenic process. In these cases, imaging VSMC proliferation, by targeting epitopes expressed on proliferating cells, provides unique information on the neointimal hyperplastic process.

Z2D3, an antibody originally discovered by screening of hybridomas generated against human atherosclerosis, displays binding specificity for VSMCs with a proliferative phenotype [130]. Derivatives of this antibody were amongst the first molecular imaging probes studied for imaging vessel wall biology [131]. Although not optimal for imaging and large-scale production, radiolabeled Z2D3 fragments have been shown to detect VSMC proliferation in coronary in-stent restenosis and transplant rejection in vivo [130, 132].

Another putative target for molecular imaging of VSMC proliferation is the integrin family of adhesion molecules. Integrins are heterodimeric surface proteins involved in cell–cell and cell–matrix adhesion. Integrins $\alpha_v\beta_3$ is upregulated and undergoes conformational change on the adluminal surface of endothelial cells as well as medial VSMCs during angiogenesis and arterial remodeling [133]. Underscoring the importance of $\alpha_v\beta_3$ integrin in vascular remodeling are reports that $\alpha_v\beta_3$ inhibition ameliorates neointima formation induced by vascular injury [134–136]. $\alpha_v\beta_3$ integrin is upregulated in injury-induced vascular remodeling and transplant vasculopathy. RP748, an ^{111}In-labeled quinolone with specificity for α_v integrins' high affinity conformation, was evaluated for detection of vascular remodeling in murine models of mechanical or immune-mediated injury. In both models, RP748 uptake in the vessel wall detected by autoradiography increased after injury and its uptake paralleled cell proliferation at different time points after injury [137, 138]. It remains to be empirically determined whether integrin-targeted probes provide sufficient signal for imaging cell proliferation in vivo.

Angiogenesis

A key feature of atherosclerosis is the angiogenic expansion of the vasa vasorum in the adventitia. Mural neovascular development accelerates lesion progression and instability by providing conduits for immune cell invasion and by increasing the foci for intraplaque hemorrhage [139–143]. Nontargeted imaging may be used to evaluate the extent of plaque vascularization using traditional imaging techniques [144–146]. However, targeted molecular imaging has the potential of detecting the angiogenic *process*. The molecular events surrounding angiogenesis involve cell proliferation, migration, and adhesion as well as matrix remodeling. The integrin family of adhesion molecules expressed on endothelial cells mediates many of these processes and has been extensively investigated as targets for molecular imaging of

angiogenesis. Integrin $\alpha_v\beta_3$ is the most commonly used target for imaging angiogenesis, although many of the probes developed to date show a broader specificity for α_v integrin. In an early study using hyperlipidemic rabbits, targeted imaging of the $\alpha_v\beta_3$ integrin using paramagnetic perfluorocarbon nanoparticle coated with an RGD-mimetic small molecule allowed noninvasive detection of atherosclerotic lesions in the aorta with MRI [147]. The enhancement signal could be blocked with nonparamagnetic nanoparticles, establishing specificity of the signal. On histological analysis, $\alpha_v\beta_3$ integrin positive vessels (present at the adventitia–media interface) constituted a fraction of all of the total vasculature detected by CD31 staining. As discussed above, in addition to endothelial cells, $\alpha_v\beta_3$ integrin is expressed by VSMCs and macrophages. The inability of bulky nanoprobes to leave the vascular space assures selective targeting of angiogenic endothelial cells with this approach. In a subsequent study, fumagillin, an antiangiogenic agent, was intercalated within the surfactant layer of the $\alpha_v\beta_3$ integrin nanoparticle such that the $\alpha_v\beta_3$ integrin probe could be used for selective drug delivery to atherosclerotic sites [148]. Repeat imaging in atherosclerotic rabbits following drug delivery showed reduced signal enhancement in fumagillin-treated animals, and histological analysis showed fewer microvessels in these animals [148]. Interestingly, while statin therapy had no long-term antivascular effect, targeted delivery of fumagillin combined with statin therapy showed a synergistic effect in decreasing integrin-mediated angiogenesis in vivo (Fig. 5.3) [149]. It is worthwhile to note that a number of other probes based on other targets (VEGF, Robo4) and imaging platforms (ultrasound) have been developed for imaging angiogenesis, and their usefulness for imaging atherosclerosis remains to be determined [150–152].

Apoptosis

Apoptosis occurs in a number of cell types within atherosclerotic lesions, and may contribute to plaque instability by enhancing the size of the necrotic core and thinning of the overlying fibrous cap [153]. Apoptosis is a regulated and energy-dependent process triggered by either extrinsic (e.g., tumor necrosis factor-α, Fas ligand) or intrinsic (e.g., free radicals, calcium) signals. During apoptosis, alterations in the cell membrane and cytoplasmic proteins occur, which may be targeted for imaging [154]. As part of the apoptotic process, the organization of the plasma membrane is altered such that phosphatidylserine, a phospholipid typically confined to the inner bilayer, becomes exposed on the outer surface [155]. Once believed to be a hallmark of apoptosis, phosphatidylserine translocation is also observed in nonapoptotic cells [156, 157].

In atherosclerosis, there is extensive macrophage apoptosis (especially in the fibrous cap) in ruptured plaques, suggesting that imaging apoptosis may help identify high risk lesions [158]. Because annexin V has high affinity for phosphatidylserine, annexin V-based agents have been investigated as probes for imaging

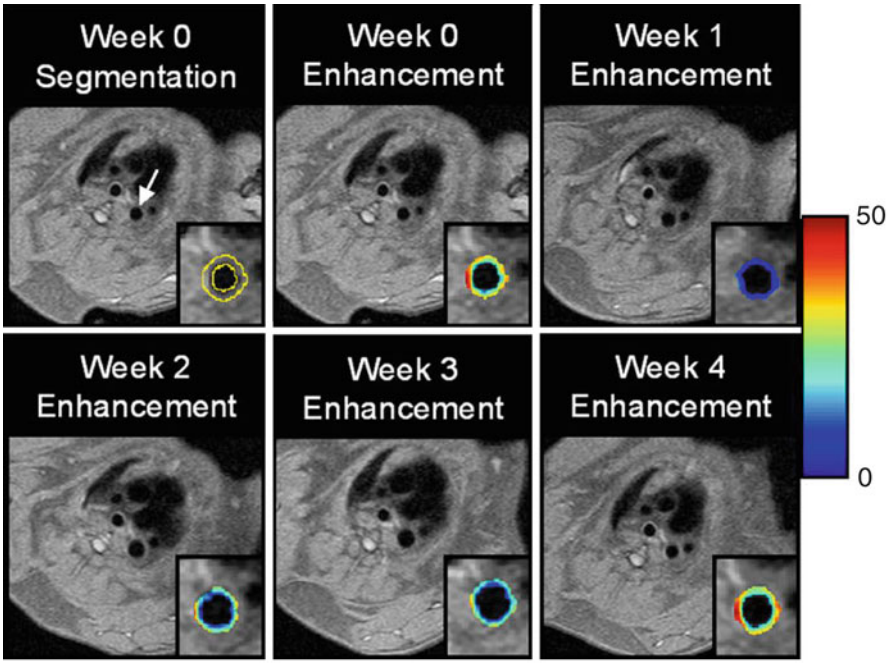

Fig. 5.3 Integrin $\alpha_v\beta_3$-targeted MRI of plaque angiogenesis and targeted fumagillin (a suppressor of angiogenesis) delivery in atherosclerotic rabbit aorta. Color-coded signal enhancement overlaid on T_1-weighted MR images demonstrating a reduction in signal enhancement 1 week after targeted fumagillin therapy. The signal enhancement of $\alpha_v\beta_3$-targeted nanoparticles subsequently gradually increases and returns to baseline level (week 0) after 4 weeks. Reprinted from [149] with permission from Elsevier

apoptosis in various pathologies [159]. In a rabbit model of atherosclerosis, planar imaging with ^{99m}Tc-annexin V demonstrated uptake of the tracer along the aorta. Tracer uptake was confirmed by autoradiography and histological analysis demonstrated enhanced tracer uptake in advanced lesions [160]. Similarly, in murine models of atherosclerosis, ^{99m}Tc-annexin V SPECT/CT imaging demonstrated areas of enhanced tracer uptake. Tracer uptake in the aorta was confirmed by autoradiography and was found to be highest in apoE$^{-/-}$ (or LDLR$^{-/-}$) mice on a high fat diet followed by apoE$^{-/-}$ (or LDLR$^{-/-}$) mice fed normal chow, and considerably less in wild-type control animals [161]. On histological analysis, tracer uptake correlated with macrophage and apoptosis immunostaining [161]. In a model of balloon injury to coronary arteries in high fat-fed swine, ^{99m}Tc-annexin V localized in a subset of injured arteries, with tracer uptake correlating with apoptosis rate quantified on histological samples [162].

Direct comparison of MMP-targeted and annexin-based imaging in rabbit [163] and murine [164] models of atherosclerosis has been performed. However, to draw

reliable conclusions, a number of technical challenges associated with dual tracer and serial imaging will need to be addressed. Ultimately, annexin imaging may not be an optimal approach as it suffers from a several major limitations for detection of apoptosis. As discussed above, phosphatidylserine translocation is not specific to apoptotic cells. Annexin V binds to several other membrane proteins unrelated to apoptosis (e.g., interferon-γ receptor [165]), and annexin V alone cannot differentiate between cell necrosis and apoptosis as loss of membrane integrity in necrosis exposes phosphatidylserine to annexin V. To overcome these limitations, alternative approaches to imaging apoptosis (e.g., targeting caspase activation) are under development [159].

Calcification

In clinical studies, arterial calcification is often used as surrogate for atherosclerosis burden. Nonetheless, vascular calcification is a complex process resembling embryonic bone formation and may take several forms. Intimal calcification is linked with atherosclerosis, while medial calcification is often observed in patients with type 2 diabetes mellitus and chronic kidney disease [166]. In atherosclerotic calcification, the presence of small calcific deposits in a spotty or speckled pattern is linked with plaque vulnerability and unstable angina, although there is considerable overlap between calcification pattern and different clinical presentations [23, 167, 168]. CT is the most commonly used imaging modality for detecting arterial calcification. However, small deposits are often missed by CT imaging. IVUS can differentiate different patterns of calcification and has been used in clinical studies to investigate potential associations with symptoms [167, 168].

Phosphonates which bind to hydroxyapatite, the major mineral product of osteoblasts, may be used for the detection of calcification. The classical example is ^{99m}Tc-methylene diphosphonate (MDP) which is used for imaging bone lesions. The development of a NIRF probe based on conjugated biphosphonates (e.g., OsteoSense750) has allowed in vivo imaging of osteoblastic activity by optical imaging [169]. When injected to atherosclerotic apoE$^{-/-}$ mice in conjunction with NIRF probes for detection of macrophages or protease activity, there was a strong correlation between OsteoSense750 and macrophage signals in different regions of the aorta, suggesting an association between the two processes. Interestingly, there was a discordance between the temporal pattern of signals from the protease and OsteoSense750 probes, with the signal from cathepsin K probe detectable in carotid arteries of 20- and 30-week-old mice, while the osteogenic signal (which did not colocalize with cathepsin K signal) was detected only at 30 weeks [170]. Importantly, NIRF imaging provided sufficient sensitivity and resolution for ex vivo detection of foci of microcalcifications in the aorta that were undetectable by microCT imaging.

Thrombosis

Plaque rupture or erosion generates a prothrombotic interface for platelet activation, adhesion, and aggregation. The platelet aggregate may progress into an occlusive thrombus, causing acute coronary syndromes or alternatively remain asymptomatic and contribute to the progression of atherosclerosis [171]. As such, imaging thrombosis (platelet-rich or organized) can be useful for assessing atherosclerosis and its consequences. Thrombus formation involves a cascade of events including platelet activation, activation of coagulation factors, conversion of fibrinogen to fibrin, and subsequent cross-linking of fibrin. The platelet-specific glycoprotein $\alpha_{IIb}\beta_3$ integrin plays an important role in platelet recruitment and aggregation at the sites of endothelial injury. Similar to $\alpha_v\beta_3$ integrin, activation of $\alpha_{IIb}\beta_3$ integrin involves conformational changes in its quaternary structure that generate high affinity binding sites for fibrinogen and von Willebrand factor [172]. These epitopes may be used as targets for imaging thrombosis. Apcitide is a ^{99m}Tc-labeled probe that binds to integrin $\alpha_{IIb}\beta_3$ on activated platelets and can be used for imaging acute deep venous thrombosis [173–175]. Similarly, MPIO conjugated to an anti-$\alpha_{IIb}\beta_3$ integrin single chain antibody can detect platelet-rich human thrombi by MRI ex vivo [176]. In a model of arachidonic acid-induced carotid thrombosis in the mouse, P975, a Gd chelate-conjugated cyclic RGD peptide targeting $\alpha_v\beta_3$ and $\alpha_{IIb}\beta_3$ was used to detect arterial thrombosis by MRI in vivo [177]. While this agent may potentially be useful for imaging plaque-associated thrombosis, the requirement for delayed (2 h) imaging to generate a specific signal excludes its use in acute settings.

Fibrin generation is another aspect of thrombosis which may be used as an imaging target. During acute thrombosis, fibrin's circulating precursor, fibrinogen, becomes selectively cleaved by activated thrombin [178]. Consequently fibrin is selectively deposited in abundant quantities over plaque-associated thrombi, making it an attractive target for molecular imaging. A gadolinium-based fibrin-specific contrast agent, termed EP2104R, has been validated in human subjects for noninvasive detection of coronary, pulmonary, and peripheral arterial thromboses by MRI [179–182]. An alternative approach to targeted imaging of thrombosis involves the activated form of coagulation factor XIII (FXIIIa) generated in the course of thrombogenesis. FXIIIa covalently cross-links α_2-antiplasmin (α_2-AP, the main inactivator of plasmin) to fibrin [183], and α_2-AP-based optical and MR probes have been used to detect arterial thrombosis in vivo [184, 185]. To date, none of the methods developed for targeted imaging of thrombosis has been shown to detect atherosclerotic plaque-associated thrombosis, and it remains to be determined if this approach is able to compete with nontargeted approaches to detect thrombosis.

Vascular Molecular Imaging in Humans

^{18}F-FDG Imaging of Vessel Wall Inflammation

As discussed earlier, ^{18}F-FDG PET imaging may be used to detect vessel wall inflammation in animal models of atherosclerosis. ^{18}F-FDG uptake in human arteries was first noted on PET studies performed for cancer staging [186]. Correlative studies demonstrated ^{18}F-FDG uptake to be associated with age, hypertension, hyperlipidemia, and smoking [187, 188]. Interestingly, vascular calcification and ^{18}F-FDG uptake rarely overlapped, suggesting the presence of distinct processes [189]. To further investigate whether plaque inflammation could be visualized and quantified noninvasively using ^{18}F-FDG PET in humans, patients with symptomatic carotid stenosis underwent ^{18}F-FDG PET imaging before carotid endarterectomy. On PET images there was approximately fourfold higher ^{18}F-FDG uptake in symptomatic carotid arteries as compared with asymptomatic contra-lateral lesions [190]. Furthermore, autoradiographic examination of carotid endarterectomy samples from symptomatic patient exposed to ^{3}H-deoxyglucose (an ^{18}F-FDG analogue) ex vivo showed predominant uptake of the tracer at the lipid core-fibrous cap border which is rich in macrophages [190]. Subsequent data demonstrated a strong correlation between ^{18}F-FDG uptake in endarterectomy samples and macrophage (CD68) staining [191] and established reproducibility of ^{18}F-FDG PET imaging in carotid arteries and aorta [192]. In patients with ^{18}F-FDG uptake in carotid arteries or aorta, repeated imaging after 3 months demonstrated a reduction in ^{18}F-FDG uptake in those treated with simvastatin compared to those who underwent dietary modification, establishing the ability of PET imaging to track the effect of therapeutic interventions on vessel wall biology [193]. Similarly, life style modification for an average of 17 months in a group of asymptomatic patients with risk factors for atherosclerosis led to a significant reduction in the number of ^{18}F-FDG-positive lesions along the great vessels. Interestingly, in this study, the changes in ^{18}F-FDG uptake best correlated with changes in high density lipoprotein (HDL) plasma levels [194].

Much of the work in this area has focused on imaging the aorta and great vessels. Cardiac motion and ^{18}F-FDG uptake by normal myocardium are impediments to imaging coronary arteries. To overcome this limitation, a number of protocols have been developed to suppress myocardial ^{18}F-FDG uptake [195]. Using this approach for cardiac ^{18}F-FDG PET imaging, a difference in target-to-background ratio between lesions culprit for acute coronary syndromes and those corresponding to stable symptoms was reported (Fig. 5.4) [196]. Despite these advances, because of cardiac motion the left main and proximal left anterior descending arteries are probably the only coronaries which can be imaged with relative accuracy using this approach.

The correlation between ^{18}F-FDG uptake on PET images and anatomical features of plaque detected by CT and MRI was investigated in a group of patients

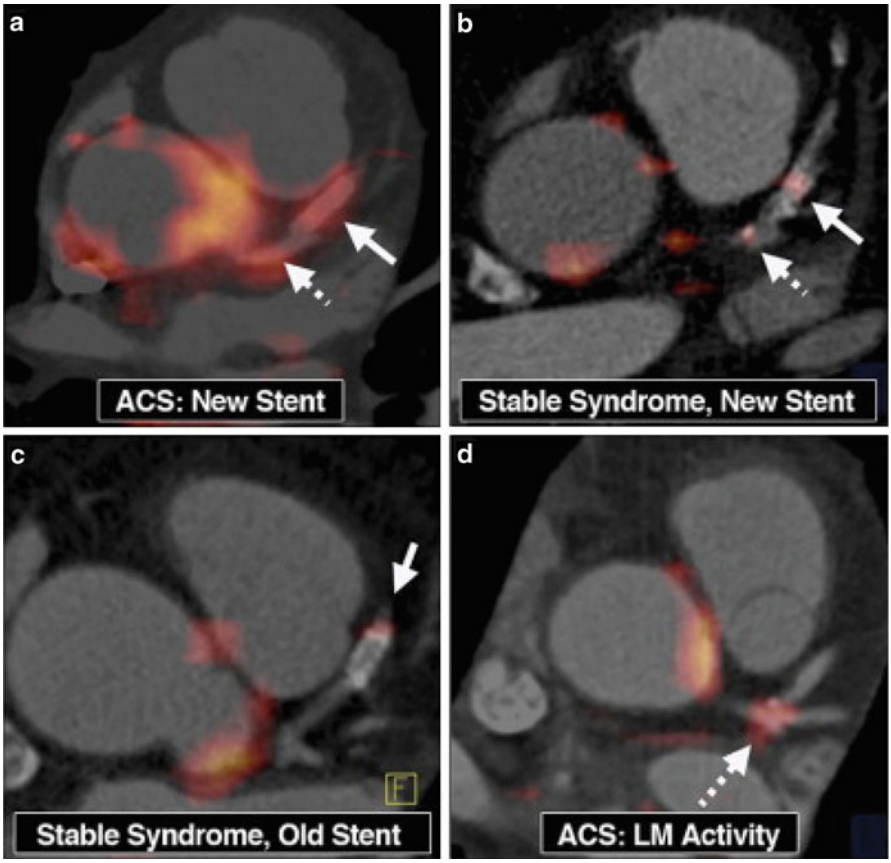

Fig. 5.4 ^{18}F-FDG PET/CT images demonstrating tracer uptake in the left main (LM) coronary artery in patients who presented with acute coronary syndrome (ACS) and uptake to a lesser degree in patients with stable syndrome. *Solid arrows* show stent locations. *Dashed arrows* show lesions within the LM. Reprinted from [196] with permission from Elsevier

with recent neurological symptoms and ipsilateral carotid stenosis. Surprisingly, there was no strong correlation between ^{18}F-FDG uptake and any CT or MRI measurement. ^{18}F-FDG uptake was higher in lesions with intraplaque hemorrhage but not in lesions with a thin or ruptured fibrous cap [197]. In another study, ^{18}F-FDG PET imaging in patients undergoing screening for carotid disease by ultrasound was positive in a subset of patients without detectable atherosclerosis. This raises questions pertaining to the source of ^{18}F-FDG uptake in carotid arteries in these patients [198]. Regarding the source of ^{18}F-FDG uptake in atherosclerosis, much of the existing literature points to macrophages. In most studies, macrophages are defined by their CD68 positive immunostaining. While the representativeness of immunostaining on random histological sections for the whole lesion may be

questioned, a study of ^{18}F-FDG PET imaging prior to endarterectomy in patients with symptomatic carotid stenosis found a similar correlation between CD68 mRNA from 3-mm-thick segments of the artery and ^{18}F-FDG uptake [199]. As a marker for macrophages, CD68 is somewhat nonspecific and may be expressed by other cells, including adipocytes [200] and lipid-loaded VSMCs [201]. Despite these limitations, ^{18}F-FDG is the most clinically advanced vascular molecular imaging probe available at the present time and is currently extensively employed to assess efficacy of antiatherosclerotic drugs in clinical trials [202].

Ultrasmall Superparamagnetic Iron Oxide Imaging of Carotid Inflammation

The relatively long blood half-life of ultrasmall superparamagnetic iron oxide (USPIO) in humans (~30 h) allows their accumulation in macrophages. This has led to their proposed use for detection of metastatic cancer in lymph nodes [203]. Preliminary studies in animals [60] and incidental uptake in atherosclerotic arteries noted on cancer staging studies [63] led to investigation of USPIO for imaging inflammation in carotid atherosclerosis. In a prospective study, patients with symptomatic carotid stenosis underwent MRI before and 24 or 72 h after USPIO (Sinerem®) administration [62]. USPIO was taken up primarily in macrophages but also in endothelial cells, myofibroblasts and VSMCs in 10 out of 11 endarterectomy samples, and MRI signal was detectable in half of these patients. USPIO uptake in carotid atherosclerosis in association with macrophages was confirmed in several follow-up studies [64, 204]. More recently, this agent was used in a prospective study to assess the effect of statin therapy on carotid inflammation. In asymptomatic patients with at least 40% carotid stenosis and USPIO signal loss on an initial MR study, treatment with high-dose atorvastatin (80 mg) for 12 weeks led to a modest, yet significant reduction in USPIO signal intensity on T_2^*-weighted MR images [205]. These changes were not observed in the low-dose treatment group receiving 20 mg daily of atorvastatin. While several major technical challenges associated with MR imaging of USPIO uptake in atherosclerosis persist [59, 206], this study provided evidence for possible use of USPIO-based MRI for assessing the effect of therapeutic interventions on atherosclerosis.

Fibrin-Specific MR Imaging of Thrombosis

In a proof of principle study, a fibrin-specific gadolinium-based contrast agent, EP-2104R, was used to detect cardiac, aortic, or carotid thrombosis by MRI [182, 207]. In addition to detecting the great majority of thrombi identified by other modalities, this approach identified additional loci of thrombus in two patients. Additional studies are needed to delineate optimal imaging parameters and the effectiveness of EP-2104R for imaging plaque-associated thrombosis.

Conclusion

Molecular imaging is critically dependent on identification of appropriate targets, development of specific and selective probes, and refinements in imaging technology. The small size of the vessel wall and cardiac motion considerably increase the challenges associated with vascular molecular imaging. A diverse range of molecules, including adhesion molecules, proteases, scavenger receptors, and clotting factors, are induced and somewhat selectively expressed in vascular pathologies and are thus putative targets for molecular imaging. While the direct exposure of endothelial cells to blood facilitate the delivery of targeted MRI and ultrasound probes to targets expressed on endothelial cells, imaging of subendothelial cell structures remain challenging for these imaging platforms. Nuclear and fluorescent imaging are particularly useful for this purpose. An important factor to keep in mind is the vastly different requirements and challenges associated with imaging in small animals (e.g., for vascular biology research) and in humans. For example, fluorescent imaging is a powerful tool for basic research studies in small animals. However, application of fluorescent imaging to imaging blood vessels in humans is currently only possible with invasive strategies. Nuclear imaging modalities (PET and SPECT) are highly quantitative in nature and appear as especially promising for clinical translation of molecular imaging. Ultimately, vascular molecular imaging will most likely be based on multimodality imaging (e.g., PET/CT) which combines the strengths and overcome the limitation of each imaging modality.

Translational studies applying molecular imaging to human disease are ongoing. Refinement of these techniques will broaden the theoretical limitations of noninvasive imaging, allowing for early identification and risk stratification of patients with coronary artery and other vascular diseases. Significant progress has already been made with regards to developing probes targeted at relevant molecular markers of vascular diseases. From an economic standpoint, ultimately those probes that target key biological processes common to several pathologies (e.g., inflammation, MMP activation) have the highest likelihood of being viable for clinical translation. Similarly, PET and SPECT are widely available and routinely used in clinical cardiovascular medicine. This increases the likelihood of their use in clinical vascular molecular imaging. Indeed, FDG PET imaging is currently under fairly advanced investigation as a tool for detecting inflammation in human carotid, coronary, and aortic disease.

When targeted imaging becomes clinically viable, its application to patient care will fundamentally alter the paradigm of management of a broad range of cardiovascular diseases including CAD, peripheral vascular disease, myocardial infarction, and aortic aneurysm. Molecular imaging will allow providers to identify at-risk patients, subsequently permitting individualization of therapies which is expected to confer efficiencies to health care delivery by identifying patients who will benefit most from costly or invasive therapies. An important application of molecular imaging is in providing early endpoints for clinical trials in vascular diseases, which can considerably shorten the time and reduce the associated costs.

In concert with established pharmacologic and invasive therapies, molecular imaging may in the future serve as an indispensable component in providers' armamentarium to diagnose and treat vascular diseases.

References

1. Stone GW, Maehara A, Lansky AJ, et al. A prospective natural-history study of coronary atherosclerosis. N Engl J Med. 2011;364:226–35.
2. Prati F, Regar E, Mintz GS, et al. Expert review document on methodology, terminology, and clinical applications of optical coherence tomography: physical principles, methodology of image acquisition, and clinical application for assessment of coronary arteries and atherosclerosis. Eur Heart J. 2010;31:401–15.
3. Thakur ML, Lentle BC. Joint SNM/RSNA molecular imaging summit statement. J Nucl Med. 2005;46:11N–13N, 42N.
4. Franc BL, Acton PD, Mari C, Hasegawa BH. Small-animal SPECT and SPECT/CT: important tools for preclinical investigation. J Nucl Med. 2008;49:1651–63.
5. Hwang AB, Franc BL, Gullberg GT, Hasegawa BH. Assessment of the sources of error affecting the quantitative accuracy of SPECT imaging in small animals. Phys Med Biol. 2008;53:2233–52.
6. Mawlawi O, Townsend DW. Multimodality imaging: an update on PET/CT technology. Eur J Nucl Med Mol Imaging. 2009;36 Suppl 1:S15–29.
7. Peng BH, Levin CS. Recent development in PET instrumentation. Curr Pharm Biotechnol. 2010;11:555–71.
8. Botnar RM, Nagel E. Structural and functional imaging by MRI. Basic Res Cardiol. 2008;103:152–60.
9. Winter PM, Caruthers SD, Lanza GM, Wickline SA. Quantitative cardiovascular magnetic resonance for molecular imaging. J Cardiovasc Magn Reson. 2010;12:62.
10. Sipkins DA, Cheresh DA, Kazemi MR, Nevin LM, Bednarski MD, Li KC. Detection of tumor angiogenesis in vivo by alphaVbeta3-targeted magnetic resonance imaging. Nat Med. 1998;4:623–6.
11. Yu X, Song SK, Chen J, et al. High-resolution MRI characterization of human thrombus using a novel fibrin-targeted paramagnetic nanoparticle contrast agent. Magn Reson Med. 2000;44:867–72.
12. Amirbekian V, Lipinski MJ, Briley-Saebo KC, et al. Detecting and assessing macrophages in vivo to evaluate atherosclerosis noninvasively using molecular MRI. Proc Natl Acad Sci U S A. 2007;104:961–6.
13. Waters EA, Wickline SA. Contrast agents for MRI. Basic Res Cardiol. 2008;103:114–21.
14. Lipinski MJ, Briley-Saebo KC, Mani V, Fayad ZA. "Positive contrast" inversion-recovery with ON[corrected]-resonant water suppression magnetic resonance imaging: a change for the better? J Am Coll Cardiol. 2008;52:492–4.
15. Villanueva FS, Wagner WR. Ultrasound molecular imaging of cardiovascular disease. Nat Clin Pract Cardiovasc Med. 2008;5 Suppl 2:S26–32.
16. Weissleder R, Ntziachristos V. Shedding light onto live molecular targets. Nat Med. 2003;9:123–8.
17. Jaffer FA, Libby P, Weissleder R. Optical and multimodality molecular imaging: insights into atherosclerosis. Arterioscler Thromb Vasc Biol. 2009;29:1017–24.
18. Chang K, Jaffer F. Advances in fluorescence imaging of the cardiovascular system. J Nucl Cardiol. 2008;15:417–28.
19. Ntziachristos V, Ripoll J, Wang LV, Weissleder R. Looking and listening to light: the evolution of whole-body photonic imaging. Nat Biotechnol. 2005;23:313–20.

20. Hyafil F, Cornily JC, Feig JE, et al. Noninvasive detection of macrophages using a nanoparticulate contrast agent for computed tomography. Nat Med. 2007;13:636–41.
21. Libby P. Inflammation in atherosclerosis. Nature. 2002;420:868–74.
22. Abrams J. Clinical practice. Chronic stable angina. N Engl J Med. 2005;352:2524–33.
23. Virmani R, Burke AP, Farb A, Kolodgie FD. Pathology of the vulnerable plaque. J Am Coll Cardiol. 2006;47:C13–8.
24. Finn AV, Nakano M, Narula J, Kolodgie FD, Virmani R. Concept of vulnerable/unstable plaque. Arterioscler Thromb Vasc Biol. 2010;30:1282–92.
25. Sadeghi MM. The pathobiology of the vessel wall: implications for imaging. J Nucl Cardiol. 2006;13:402–14.
26. Cybulsky MI, Gimbrone Jr MA. Endothelial expression of a mononuclear leukocyte adhesion molecule during atherogenesis. Science. 1991;251:788–91.
27. Sadeghi MM, Schechner JS, Krassilnikova S, et al. Vascular cell adhesion molecule-1-targeted detection of endothelial activation in human microvasculature. Transplant Proc. 2004;36:1585–91.
28. McAteer MA, Sibson NR, von Zur Muhlen C, et al. In vivo magnetic resonance imaging of acute brain inflammation using microparticles of iron oxide. Nat Med. 2007;13:1253–8.
29. Kelly KA, Allport JR, Tsourkas A, Shinde-Patil VR, Josephson L, Weissleder R. Detection of vascular adhesion molecule-1 expression using a novel multimodal nanoparticle. Circ Res. 2005;96:327–36.
30. Kelly KA, Nahrendorf M, Yu AM, Reynolds F, Weissleder R. In vivo phage display selection yields atherosclerotic plaque targeted peptides for imaging. Mol Imaging Biol. 2006;8:201–7.
31. Nahrendorf M, Jaffer FA, Kelly KA, et al. Noninvasive vascular cell adhesion molecule-1 imaging identifies inflammatory activation of cells in atherosclerosis. Circulation. 2006;114:1504–11.
32. Nahrendorf M, Keliher E, Panizzi P, et al. 18F-4V for PET-CT imaging of VCAM-1 expression in atherosclerosis. JACC Cardiovasc Imaging. 2009;2:1213–22.
33. Villanueva FS, Jankowski RJ, Klibanov S, et al. Microbubbles targeted to intercellular adhesion molecule-1 bind to activated coronary artery endothelial cells. Circulation. 1998;98:1–5.
34. Kaufmann BA, Sanders JM, Davis C, et al. Molecular imaging of inflammation in atherosclerosis with targeted ultrasound detection of vascular cell adhesion molecule-1. Circulation. 2007;116:276–84.
35. Kaufmann BA, Carr CL, Belcik JT, et al. Molecular imaging of the initial inflammatory response in atherosclerosis: implications for early detection of disease. Arterioscler Thromb Vasc Biol. 2010;30:54–9.
36. Reynolds PR, Larkman DJ, Haskard DO, Hajnal JV, Kennea NL, George AJ, Edwards AD. Detection of vascular expression of E-selectin in vivo with MR imaging. Radiology. 2006;241:469–76.
37. van Kasteren SI, Campbell SJ, Serres S, Anthony DC, Sibson NR, Davis BG. Glyconanoparticles allow pre-symptomatic in vivo imaging of brain disease. Proc Natl Acad Sci U S A. 2009;106:18–23.
38. Sipkins DA, Gijbels K, Tropper FD, Bednarski M, Li KC, Steinman L. ICAM-1 expression in autoimmune encephalitis visualized using magnetic resonance imaging. J Neuroimmunol. 2000;104:1–9.
39. Takaya N, Yuan C, Chu B, et al. Association between carotid plaque characteristics and subsequent ischemic cerebrovascular events: a prospective assessment with MRI—initial results. Stroke. 2006;37:818–23.
40. Demarco JK, Ota H, Underhill HR, et al. MR carotid plaque imaging and contrast-enhanced MR angiography identifies lesions associated with recent ipsilateral thromboembolic symptoms: an in vivo study at 3T. AJNR Am J Neuroradiol. 2010;31:1395–402.
41. Mathiesen EB, Bonaa KH, Joakimsen O. Echolucent plaques are associated with high risk of ischemic cerebrovascular events in carotid stenosis: the tromso study. Circulation. 2001;103:2171–5.

42. Gronholdt ML, Nordestgaard BG, Schroeder TV, Vorstrup S, Sillesen H. Ultrasonic echolucent carotid plaques predict future strokes. Circulation. 2001;104:68–73.
43. Toussaint JF, LaMuraglia GM, Southern JF, Fuster V, Kantor HL. Magnetic resonance images lipid, fibrous, calcified, hemorrhagic, and thrombotic components of human atherosclerosis in vivo. Circulation. 1996;94:932–8.
44. Motoyama S, Sarai M, Harigaya H, et al. Computed tomographic angiography characteristics of atherosclerotic plaques subsequently resulting in acute coronary syndrome. J Am Coll Cardiol. 2009;54:49–57.
45. Roberts AB, Lees AM, Lees RS, et al. Selective accumulation of low density lipoproteins in damaged arterial wall. J Lipid Res. 1983;24:1160–7.
46. Rosen JM, Butler SP, Meinken GE, et al. Indium-111-labeled LDL: a potential agent for imaging atherosclerotic disease and lipoprotein biodistribution. J Nucl Med. 1990;31:343–50.
47. Lees AM, Lees RS, Schoen FJ, et al. Imaging human atherosclerosis with 99mTc-labeled low density lipoproteins. Arteriosclerosis. 1988;8:461–70.
48. Nielsen LB, Stender S, Kjeldsen K, Nordestgaard BG. Specific accumulation of lipoprotein(a) in balloon-injured rabbit aorta in vivo. Circ Res. 1996;78:615–26.
49. Iuliano L, Signore A, Vallabajosula S, et al. Preparation and biodistribution of 99m technetium labelled oxidized LDL in man. Atherosclerosis. 1996;126:131–41.
50. Tsimikas S, Palinski W, Halpern SE, Yeung DW, Curtiss LK, Witztum JL. Radiolabeled MDA2, an oxidation-specific, monoclonal antibody, identifies native atherosclerotic lesions in vivo. J Nucl Cardiol. 1999;6:41–53.
51. Tsimikas S, Shortal BP, Witztum JL, Palinski W. In vivo uptake of radiolabeled MDA2, an oxidation-specific monoclonal antibody, provides an accurate measure of atherosclerotic lesions rich in oxidized LDL and is highly sensitive to their regression. Arterioscler Thromb Vasc Biol. 2000;20:689–97.
52. Torzewski M, Shaw PX, Han KR, et al. Reduced in vivo aortic uptake of radiolabeled oxidation-specific antibodies reflects changes in plaque composition consistent with plaque stabilization. Arterioscler Thromb Vasc Biol. 2004;24:2307–12.
53. Briley-Saebo KC, Shaw PX, Mulder WJ, et al. Targeted molecular probes for imaging atherosclerotic lesions with magnetic resonance using antibodies that recognize oxidation-specific epitopes. Circulation. 2008;117:3206–15.
54. Briley-Saebo KC, Cho YS, Shaw PX, et al. Targeted iron oxide particles for in vivo magnetic resonance detection of atherosclerotic lesions with antibodies directed to oxidation-specific epitopes. J Am Coll Cardiol. 2011;57:337–47.
55. Chang MK, Binder CJ, Miller YI, et al. Apoptotic cells with oxidation-specific epitopes are immunogenic and proinflammatory. J Exp Med. 2004;200:1359–70.
56. Swirski FK, Pittet MJ, Kircher MF, et al. Monocyte accumulation in mouse atherogenesis is progressive and proportional to extent of disease. Proc Natl Acad Sci U S A. 2006;103:10340–5.
57. Kircher MF, Grimm J, Swirski FK, et al. Noninvasive in vivo imaging of monocyte trafficking to atherosclerotic lesions. Circulation. 2008;117:388–95.
58. Hartung D, Petrov A, Haider N, et al. Radiolabeled monocyte chemotactic protein 1 for the detection of inflammation in experimental atherosclerosis. J Nucl Med. 2007;48:1816–21.
59. Tang TY, Muller KH, Graves MJ, et al. Iron oxide particles for atheroma imaging. Arterioscler Thromb Vasc Biol. 2009;29:1001–8.
60. Schmitz SA, Coupland SE, Gust R, et al. Superparamagnetic iron oxide-enhanced MRI of atherosclerotic plaques in Watanabe hereditable hyperlipidemic rabbits. Invest Radiol. 2000;35:460–71.
61. Ruehm SG, Corot C, Vogt P, Kolb S, Debatin JF. Magnetic resonance imaging of atherosclerotic plaque with ultrasmall superparamagnetic particles of iron oxide in hyperlipidemic rabbits. Circulation. 2001;103:415–22.
62. Kooi ME, Cappendijk VC, Cleutjens KB, et al. Accumulation of ultrasmall superparamagnetic particles of iron oxide in human atherosclerotic plaques can be detected by in vivo magnetic resonance imaging. Circulation. 2003;107:2453–8.

63. Schmitz SA, Taupitz M, Wagner S, Wolf KJ, Beyersdorff D, Hamm B. Magnetic resonance imaging of atherosclerotic plaques using superparamagnetic iron oxide particles. J Magn Reson Imaging. 2001;14:355–61.
64. Trivedi RA, U-King-Im JM, Graves MJ, et al. In vivo detection of macrophages in human carotid atheroma: temporal dependence of ultrasmall superparamagnetic particles of iron oxide-enhanced MRI. Stroke. 2004;35:1631–5.
65. Jaffer FA, Nahrendorf M, Sosnovik D, Kelly KA, Aikawa E, Weissleder R. Cellular imaging of inflammation in atherosclerosis using magnetofluorescent nanomaterials. Mol Imaging. 2006;5:85–92.
66. Nahrendorf M, Zhang H, Hembrador S, et al. Nanoparticle PET-CT imaging of macrophages in inflammatory atherosclerosis. Circulation. 2008;117:379–87.
67. Hyafil F, Cornily JC, Rudd JH, Machac J, Feldman LJ, Fayad ZA. Quantification of inflammation within rabbit atherosclerotic plaques using the macrophage-specific CT contrast agent N1177: a comparison with 18F-FDG PET/CT and histology. J Nucl Med. 2009;50:959–65.
68. Pluddemann A, Neyen C, Gordon S. Macrophage scavenger receptors and host-derived ligands. Methods. 2007;43:207–17.
69. Greaves DR, Gordon S. Thematic review series: the immune system and atherogenesis. Recent insights into the biology of macrophage scavenger receptors. J Lipid Res. 2005;46:11–20.
70. Geng Y, Kodama T, Hansson GK. Differential expression of scavenger receptor isoforms during monocyte-macrophage differentiation and foam cell formation. Arterioscler Thromb. 1994;14:798–806.
71. Kume N, Murase T, Moriwaki H, et al. Inducible expression of lectin-like oxidized LDL receptor-1 in vascular endothelial cells. Circ Res. 1998;83:322–7.
72. Murase T, Kume N, Korenaga R, et al. Fluid shear stress transcriptionally induces lectin-like oxidized LDL receptor-1 in vascular endothelial cells. Circ Res. 1998;83:328–33.
73. Yoshida H, Kondratenko N, Green S, Steinberg D, Quehenberger O. Identification of the lectin-like receptor for oxidized low-density lipoprotein in human macrophages and its potential role as a scavenger receptor. Biochem J. 1998;334(Pt 1):9–13.
74. Ishino S, Mukai T, Kuge Y, et al. Targeting of lectinlike oxidized low-density lipoprotein receptor 1 (LOX-1) with 99mTc-labeled anti-LOX-1 antibody: potential agent for imaging of vulnerable plaque. J Nucl Med. 2008;49:1677–85.
75. Li D, Patel AR, Klibanov AL, et al. Molecular imaging of atherosclerotic plaques targeted to oxidized LDL receptor LOX-1 by SPECT/CT and magnetic resonance. Circ Cardiovasc Imaging. 2010;3:464–72.
76. Rudd JH, Narula J, Strauss HW, et al. Imaging atherosclerotic plaque inflammation by fluorodeoxyglucose with positron emission tomography: ready for prime time? J Am Coll Cardiol. 2010;55:2527–35.
77. Deichen JT, Prante O, Gack M, Schmiedehausen K, Kuwert T. Uptake of [18F]fluorodeoxyglucose in human monocyte-macrophages in vitro. Eur J Nucl Med Mol Imaging. 2003;30:267–73.
78. Newsholme P, Curi R, Gordon S, Newsholme EA. Metabolism of glucose, glutamine, long-chain fatty acids and ketone bodies by murine macrophages. Biochem J. 1986;239:121–5.
79. Maschauer S, Prante O, Hoffmann M, Deichen JT, Kuwert T. Characterization of 18F-FDG uptake in human endothelial cells in vitro. J Nucl Med. 2004;45:455–60.
80. Lederman RJ, Raylman RR, Fisher SJ, et al. Detection of atherosclerosis using a novel positron-sensitive probe and 18-fluorodeoxyglucose (FDG). Nucl Med Commun. 2001;22:747–53.
81. Ogawa M, Ishino S, Mukai T, et al. (18)F-FDG accumulation in atherosclerotic plaques: immunohistochemical and PET imaging study. J Nucl Med. 2004;45:1245–50.
82. Tawakol A, Migrino RQ, Hoffmann U, et al. Noninvasive in vivo measurement of vascular inflammation with F-18 fluorodeoxyglucose positron emission tomography. J Nucl Cardiol. 2005;12:294–301.

83. Aziz K, Berger K, Claycombe K, Huang R, Patel R, Abela GS. Noninvasive detection and localization of vulnerable plaque and arterial thrombosis with computed tomography angiography/positron emission tomography. Circulation. 2008;117:2061–70.
84. Ogawa M, Magata Y, Kato T, et al. Application of 18F-FDG PET for monitoring the therapeutic effect of antiinflammatory drugs on stabilization of vulnerable atherosclerotic plaques. J Nucl Med. 2006;47:1845–50.
85. Zhao Y, Kuge Y, Zhao S, Strauss HW, Blankenberg FG, Tamaki N. Prolonged high-fat feeding enhances aortic 18F-FDG and 99mTc-annexin A5 uptake in apolipoprotein E-deficient and wild-type C57BL/6J mice. J Nucl Med. 2008;49:1707–14.
86. Laurberg JM, Olsen AK, Hansen SB, et al. Imaging of vulnerable atherosclerotic plaques with FDG-microPET: no FDG accumulation. Atherosclerosis. 2007;192:275–82.
87. Laitinen I, Marjamaki P, Haaparanta M, et al. Non-specific binding of [18F]FDG to calcifications in atherosclerotic plaques: experimental study of mouse and human arteries. Eur J Nucl Med Mol Imaging. 2006;33:1461–7.
88. Laitinen I, Saraste A, Weidl E, et al. Evaluation of alphavbeta3 integrin-targeted positron emission tomography tracer 18F-galacto-RGD for imaging of vascular inflammation in atherosclerotic mice. Circ Cardiovasc Imaging. 2009;2:331–8.
89. Waldeck J, Hager F, Holtke C, et al. Fluorescence reflectance imaging of macrophage-rich atherosclerotic plaques using an alphavbeta3 integrin-targeted fluorochrome. J Nucl Med. 2008;49:1845–51.
90. Varnava AM, Mills PG, Davies MJ. Relationship between coronary artery remodeling and plaque vulnerability. Circulation. 2002;105:939–43.
91. Pasterkamp G, Fitzgerald PF, de Kleijn DP. Atherosclerotic expansive remodeled plaques: a wolf in sheep's clothing. J Vasc Res. 2002;39:514–23.
92. Kataoka T, Mathew V, Rubinshtein R, et al. Association of plaque composition and vessel remodeling in atherosclerotic renal artery stenosis: a comparison with coronary artery disease. JACC Cardiovasc Imaging. 2009;2:327–38.
93. van Goor H, Melenhorst WB, Turner AJ, Holgate ST. Adamalysins in biology and disease. J Pathol. 2009;219:277–86.
94. Galis ZS, Khatri JJ. Matrix metalloproteinases in vascular remodeling and atherogenesis: the good, the bad, and the ugly. Circ Res. 2002;90:251–62.
95. Lutgens SP, Cleutjens KB, Daemen MJ, Heeneman S. Cathepsin cysteine proteases in cardiovascular disease. FASEB J. 2007;21:3029–41.
96. Nicholl SM, Roztocil E, Davies MG. Plasminogen activator system and vascular disease. Curr Vasc Pharmacol. 2006;4:101–16.
97. Hadler-Olsen E, Fadnes B, Sylte I, Uhlin-Hansen L, Winberg JO. Regulation of matrix metalloproteinase activity in health and disease. FEBS J. 2011;278:28–45.
98. Back M, Ketelhuth DF, Agewall S. Matrix metalloproteinases in atherothrombosis. Prog Cardiovasc Dis. 2010;52:410–28.
99. Dollery CM, Libby P. Atherosclerosis and proteinase activation. Cardiovasc Res. 2006;69:625–35.
100. Newby AC. Dual role of matrix metalloproteinases (matrixins) in intimal thickening and atherosclerotic plaque rupture. Physiol Rev. 2005;85:1–31.
101. Johnson JL, George SJ, Newby AC, Jackson CL. Divergent effects of matrix metalloproteinases 3, 7, 9, and 12 on atherosclerotic plaque stability in mouse brachiocephalic arteries. Proc Natl Acad Sci U S A. 2005;102:15575–80.
102. Funovics M, Weissleder R, Tung CH. Protease sensors for bioimaging. Anal Bioanal Chem. 2003;377:956–63.
103. Deguchi JO, Aikawa M, Tung CH, et al. Inflammation in atherosclerosis: visualizing matrix metalloproteinase action in macrophages in vivo. Circulation. 2006;114:55–62.
104. Kaijzel EL, van Heijningen PM, Wielopolski PA, et al. Multimodality imaging reveals a gradual increase in matrix metalloproteinase activity at aneurysmal lesions in live fibulin-4 mice. Circ Cardiovasc Imaging. 2010;3:567–77.

105. Jiang T, Olson ES, Nguyen QT, Roy M, Jennings PA, Tsien RY. Tumor imaging by means of proteolytic activation of cell-penetrating peptides. Proc Natl Acad Sci U S A. 2004;101: 17867–72.
106. van Duijnhoven SM, Robillard MS, Nicolay K, Grull H. Tumor targeting of MMP-2/9 activatable cell-penetrating imaging probes is caused by tumor-independent activation. J Nucl Med. 2011;52:279–86.
107. Schafers M, Riemann B, Kopka K, et al. Scintigraphic imaging of matrix metalloproteinase activity in the arterial wall in vivo. Circulation. 2004;109:2554–9.
108. Zhang J, Nie L, Razavian M, et al. Molecular imaging of activated matrix metalloproteinases in vascular remodeling. Circulation. 2008;118:1953–60.
109. Tavakoli S, Razavian M, Zhang J, et al. Matrix metalloproteinase activation predicts amelioration of remodeling after dietary modification in injured arteries. Arterioscler Thromb Vasc Biol. 2011;31:102–9.
110. Razavian M, Zhang J, Nie L, et al. Molecular imaging of matrix metalloproteinase activation to predict murine aneurysm expansion in vivo. J Nucl Med. 2010;51:1107–15.
111. Fujimoto S, Hartung D, Ohshima S, et al. Molecular imaging of matrix metalloproteinase in atherosclerotic lesions: resolution with dietary modification and statin therapy. J Am Coll Cardiol. 2008;52:1847–57.
112. Ohshima S, Fujimoto S, Petrov A, et al. Effect of an antimicrobial agent on atherosclerotic plaques: assessment of metalloproteinase activity by molecular imaging. J Am Coll Cardiol. 2011;55:1240–9.
113. Ohshima S, Petrov A, Fujimoto S, et al. Molecular imaging of matrix metalloproteinase expression in atherosclerotic plaques of mice deficient in apolipoprotein e or low-density-lipoprotein receptor. J Nucl Med. 2009;50:612–7.
114. Lancelot E, Amirbekian V, Brigger I, et al. Evaluation of matrix metalloproteinases in atherosclerosis using a novel noninvasive imaging approach. Arterioscler Thromb Vasc Biol. 2008;28:425–32.
115. Amirbekian V, Aguinaldo JG, Amirbekian S, et al. Atherosclerosis and matrix metalloproteinases: experimental molecular MR imaging in vivo. Radiology. 2009;251:429–38.
116. Hyafil F, Vucic E, Cornily JC, et al. Monitoring of arterial wall remodelling in atherosclerotic rabbits with a magnetic resonance imaging contrast agent binding to matrix metalloproteinases. Eur Heart J. 2011;32:1561–71.
117. Bazeli R, Coutard M, Duport BD, et al. In vivo evaluation of a new magnetic resonance imaging contrast agent (P947) to target matrix metalloproteinases in expanding experimental abdominal aortic aneurysms. Invest Radiol. 2011;45:662–8.
118. Liu J, Sukhova GK, Sun JS, Xu WH, Libby P, Shi GP. Lysosomal cysteine proteases in atherosclerosis. Arterioscler Thromb Vasc Biol. 2004;24:1359–66.
119. Sukhova GK, Zhang Y, Pan JH, et al. Deficiency of cathepsin S reduces atherosclerosis in LDL receptor-deficient mice. J Clin Invest. 2003;111:897–906.
120. Rodgers KJ, Watkins DJ, Miller AL, et al. Destabilizing role of cathepsin S in murine atherosclerotic plaques. Arterioscler Thromb Vasc Biol. 2006;26:851–6.
121. Weissleder R, Tung CH, Mahmood U, Bogdanov Jr A. In vivo imaging of tumors with protease-activated near-infrared fluorescent probes. Nat Biotechnol. 1999;17:375–8.
122. Chen J, Tung CH, Mahmood U, et al. In vivo imaging of proteolytic activity in atherosclerosis. Circulation. 2002;105:2766–71.
123. Kim DE, Kim JY, Schellingerhout D, et al. Protease imaging of human atheromata captures molecular information of atherosclerosis, complementing anatomic imaging. Arterioscler Thromb Vasc Biol. 2010;30:449–56.
124. Jaffer FA, Kim DE, Quinti L, et al. Optical visualization of cathepsin K activity in atherosclerosis with a novel, protease-activatable fluorescence sensor. Circulation. 2007;115:2292–8.
125. Nahrendorf M, Waterman P, Thurber G, et al. Hybrid in vivo FMT-CT imaging of protease activity in atherosclerosis with customized nanosensors. Arterioscler Thromb Vasc Biol. 2009;29:1444–51.
126. Jaffer FA, Vinegoni C, John MC, et al. Real-time catheter molecular sensing of inflammation in proteolytically active atherosclerosis. Circulation. 2008;118:1802–9.

127. Sheth RA, Tam JM, Maricevich MA, Josephson L, Mahmood U. Quantitative endovascular fluorescence-based molecular imaging through blood of arterial wall inflammation. Radiology. 2009;251:813–21.
128. Matter CM, Schuler PK, Alessi P, et al. Molecular imaging of atherosclerotic plaques using a human antibody against the extra-domain B of fibronectin. Circ Res. 2004;95:1225–33.
129. Dzau VJ, Braun-Dullaeus RC, Sedding DG. Vascular proliferation and atherosclerosis: new perspectives and therapeutic strategies. Nat Med. 2002;8:1249–56.
130. Johnson LL, Schofield LM, Verdesca SA, et al. In vivo uptake of radiolabeled antibody to proliferating smooth muscle cells in a swine model of coronary stent restenosis. J Nucl Med. 2000;41:1535–40.
131. Narula J, Petrov A, Bianchi C, et al. Noninvasive localization of experimental atherosclerotic lesions with mouse/human chimeric Z2D3 F(ab′)2 specific for the proliferating smooth muscle cells of human atheroma. Imaging with conventional and negative charge-modified antibody fragments. Circulation. 1995;92:474–84.
132. Jimenez J, Donahay T, Schofield L, Khaw BA, Johnson LL. Smooth muscle cell proliferation index correlates with 111In-labeled antibody Z2D3 uptake in a transplant vasculopathy swine model. J Nucl Med. 2005;46:514–9.
133. Cox D, Brennan M, Moran N. Integrins as therapeutic targets: lessons and opportunities. Nat Rev Drug Discov. 2010;9:804–20.
134. Choi ET, Engel L, Callow AD, et al. Inhibition of neointimal hyperplasia by blocking alpha V beta 3 integrin with a small peptide antagonist GpenGRGDSPCA. J Vasc Surg. 1994;19:125–34.
135. Matsuno H, Stassen JM, Vermylen J, Deckmyn H. Inhibition of integrin function by a cyclic RGD-containing peptide prevents neointima formation. Circulation. 1994;90:2203–6.
136. Srivatsa SS, Fitzpatrick LA, Tsao PW, et al. Selective alpha v beta 3 integrin blockade potently limits neointimal hyperplasia and lumen stenosis following deep coronary arterial stent injury: evidence for the functional importance of integrin alpha v beta 3 and osteopontin expression during neointima formation. Cardiovasc Res. 1997;36:408–28.
137. Sadeghi MM, Krassilnikova S, Zhang J, et al. Detection of injury-induced vascular remodeling by targeting activated alphavbeta3 integrin in vivo. Circulation. 2004;110:84–90.
138. Zhang J, Krassilnikova S, Gharaei AA, et al. Alphavbeta3-targeted detection of arteriopathy in transplanted human coronary arteries: an autoradiographic study. FASEB J. 2005;19:1857–9.
139. Moreno PR, Purushothaman KR, Fuster V, et al. Plaque neovascularization is increased in ruptured atherosclerotic lesions of human aorta: implications for plaque vulnerability. Circulation. 2004;110:2032–8.
140. Tenaglia AN, Peters KG, Sketch Jr MH, Annex BH. Neovascularization in atherectomy specimens from patients with unstable angina: implications for pathogenesis of unstable angina. Am Heart J. 1998;135:10–4.
141. Kolodgie FD, Gold HK, Burke AP, et al. Intraplaque hemorrhage and progression of coronary atheroma. N Engl J Med. 2003;349:2316–25.
142. Virmani R, Kolodgie FD, Burke AP, et al. Atherosclerotic plaque progression and vulnerability to rupture: angiogenesis as a source of intraplaque hemorrhage. Arterioscler Thromb Vasc Biol. 2005;25:2054–61.
143. Gossl M, Versari D, Hildebrandt HA, et al. Segmental heterogeneity of vasa vasorum neovascularization in human coronary atherosclerosis. JACC Cardiovasc Imaging. 2010;3:32–40.
144. Calcagno C, Mani V, Ramachandran S, Fayad ZA. Dynamic contrast enhanced (DCE) magnetic resonance imaging (MRI) of atherosclerotic plaque angiogenesis. Angiogenesis. 2010;13:87–99.
145. Kwon HM, Sangiorgi G, Ritman EL, et al. Adventitial vasa vasorum in balloon-injured coronary arteries: visualization and quantitation by a microscopic three-dimensional computed tomography technique. J Am Coll Cardiol. 1998;32:2072–9.
146. Giannarelli C, Ibanez B, Cimmino G, et al. Contrast-enhanced ultrasound imaging detects intraplaque neovascularization in an experimental model of atherosclerosis. JACC Cardiovasc Imaging. 2010;3:1256–64.
147. Winter PM, Morawski AM, Caruthers SD, et al. Molecular imaging of angiogenesis in early-stage atherosclerosis with alpha(v)beta3-integrin-targeted nanoparticles. Circulation. 2003; 108:2270–4.

148. Winter PM, Neubauer AM, Caruthers SD, et al. Endothelial alpha(v)beta3 integrin-targeted fumagillin nanoparticles inhibit angiogenesis in atherosclerosis. Arterioscler Thromb Vasc Biol. 2006;26:2103–9.
149. Winter PM, Caruthers SD, Zhang H, Williams TA, Wickline SA, Lanza GM. Antiangiogenic synergism of integrin-targeted fumagillin nanoparticles and atorvastatin in atherosclerosis. JACC Cardiovasc Imaging. 2008;1:624–34.
150. Leong-Poi H, Christiansen J, Klibanov AL, Kaul S, Lindner JR. Noninvasive assessment of angiogenesis by ultrasound and microbubbles targeted to alpha(v)-integrins. Circulation. 2003;107:455–60.
151. Rodriguez-Porcel M, Cai W, Gheysens O, et al. Imaging of VEGF receptor in a rat myocardial infarction model using PET. J Nucl Med. 2008;49:667–73.
152. Boles KS, Schmieder AH, Koch AW, et al. MR angiogenesis imaging with Robo4- vs. alphaVbeta3-targeted nanoparticles in a B16/F10 mouse melanoma model. FASEB J. 2010;24:4262–70.
153. Tabas I. Macrophage death and defective inflammation resolution in atherosclerosis. Nat Rev Immunol. 2010;10:36–46.
154. De Saint-Hubert M, Prinsen K, Mortelmans L, Verbruggen A, Mottaghy FM. Molecular imaging of cell death. Methods. 2009;48:178–87.
155. Fadok VA, Voelker DR, Campbell PA, Cohen JJ, Bratton DL, Henson PM. Exposure of phosphatidylserine on the surface of apoptotic lymphocytes triggers specific recognition and removal by macrophages. J Immunol. 1992;148:2207–16.
156. Smrz D, Draberova L, Draber P. Non-apoptotic phosphatidylserine externalization induced by engagement of glycosylphosphatidylinositol-anchored proteins. J Biol Chem. 2007;282:10487–97.
157. Elliott JI, Surprenant A, Marelli-Berg FM, et al. Membrane phosphatidylserine distribution as a non-apoptotic signalling mechanism in lymphocytes. Nat Cell Biol. 2005;7:808–16.
158. Kolodgie FD, Narula J, Burke AP, et al. Localization of apoptotic macrophages at the site of plaque rupture in sudden coronary death. Am J Pathol. 2000;157:1259–68.
159. Blankenberg FG. In vivo detection of apoptosis. J Nucl Med. 2008;49 Suppl 2:81S–95.
160. Kolodgie FD, Petrov A, Virmani R, et al. Targeting of apoptotic macrophages and experimental atheroma with radiolabeled annexin V: a technique with potential for noninvasive imaging of vulnerable plaque. Circulation. 2003;108:3134–9.
161. Isobe S, Tsimikas S, Zhou J, et al. Noninvasive imaging of atherosclerotic lesions in apolipoprotein E-deficient and low-density-lipoprotein receptor-deficient mice with annexin A5. J Nucl Med. 2006;47:1497–505.
162. Johnson LL, Schofield L, Donahay T, Narula N, Narula J. 99mTc-annexin V imaging for in vivo detection of atherosclerotic lesions in porcine coronary arteries. J Nucl Med. 2005;46:1186–93.
163. Haider N, Hartung D, Fujimoto S, et al. Dual molecular imaging for targeting metalloproteinase activity and apoptosis in atherosclerosis: molecular imaging facilitates understanding of pathogenesis. J Nucl Cardiol. 2009;16:753–62.
164. Tekabe Y, Li Q, Luma J, et al. Noninvasive monitoring the biology of atherosclerotic plaque development with radiolabeled annexin V and matrix metalloproteinase inhibitor in spontaneous atherosclerotic mice. J Nucl Cardiol. 2010;17:1073–81.
165. Leon C, Nandan D, Lopez M, Moeenrezakhanlou A, Reiner NE. Annexin V associates with the IFN-gamma receptor and regulates IFN-gamma signaling. J Immunol. 2006;176:5934–42.
166. Demer LL, Tintut Y. Vascular calcification: pathobiology of a multifaceted disease. Circulation. 2008;117:2938–48.
167. Beckman JA, Ganz J, Creager MA, Ganz P, Kinlay S. Relationship of clinical presentation and calcification of culprit coronary artery stenoses. Arterioscler Thromb Vasc Biol. 2001;21:1618–22.
168. Ehara S, Kobayashi Y, Yoshiyama M, et al. Spotty calcification typifies the culprit plaque in patients with acute myocardial infarction: an intravascular ultrasound study. Circulation. 2004;110:3424–9.

169. Zaheer A, Lenkinski RE, Mahmood A, Jones AG, Cantley LC, Frangioni JV. In vivo near-infrared fluorescence imaging of osteoblastic activity. Nat Biotechnol. 2001;19:1148–54.
170. Aikawa E, Nahrendorf M, Figueiredo JL, et al. Osteogenesis associates with inflammation in early-stage atherosclerosis evaluated by molecular imaging in vivo. Circulation. 2007; 116:2841–50.
171. Gawaz M, Langer H, May AE. Platelets in inflammation and atherogenesis. J Clin Invest. 2005;115:3378–84.
172. Furie B, Furie BC. Mechanisms of thrombus formation. N Engl J Med. 2008;359:938–49.
173. Taillefer R, Edell S, Innes G, Lister-James J. Acute thromboscintigraphy with (99m) Tc-apcitide: results of the phase 3 multicenter clinical trial comparing 99mTc-apcitide scintigraphy with contrast venography for imaging acute DVT. Multicenter Trial Investigators. J Nucl Med. 2000;41:1214–23.
174. Bates SM, Lister-James J, Julian JA, Taillefer R, Moyer BR, Ginsberg JS. Imaging characteristics of a novel technetium Tc 99m-labeled platelet glycoprotein IIb/IIIa receptor antagonist in patients with acute deep vein thrombosis or a history of deep vein thrombosis. Arch Intern Med. 2003;163:452–6.
175. Dunzinger A, Hafner F, Schaffler G, Piswanger-Soelkner JC, Brodmann M, Lipp RW. 99mTc-apcitide scintigraphy in patients with clinically suspected deep venous thrombosis and pulmonary embolism. Eur J Nucl Med Mol Imaging. 2008;35:2082–7.
176. von Zur Muhlen C, von Elverfeldt D, Choudhury RP, et al. Functionalized magnetic resonance contrast agent selectively binds to glycoprotein IIb/IIIa on activated human platelets under flow conditions and is detectable at clinically relevant field strengths. Mol Imaging. 2008;7:59–67.
177. Klink A, Lancelot E, Ballet S, et al. Magnetic resonance molecular imaging of thrombosis in an arachidonic acid mouse model using an activated platelet targeted probe. Arterioscler Thromb Vasc Biol. 2010;30:403–10.
178. Iwaki T, Ploplis VA, Castellino FJ. The hemostasis system in murine atherosclerosis. Curr Drug Targets. 2008;9:229–38.
179. Botnar RM, Buecker A, Wiethoff AJ, et al. In vivo magnetic resonance imaging of coronary thrombosis using a fibrin-binding molecular magnetic resonance contrast agent. Circulation. 2004;110:1463–6.
180. Spuentrup E, Buecker A, Katoh M, et al. Molecular magnetic resonance imaging of coronary thrombosis and pulmonary emboli with a novel fibrin-targeted contrast agent. Circulation. 2005;111:1377–82.
181. Sirol M, Fuster V, Badimon JJ, et al. Chronic thrombus detection with in vivo magnetic resonance imaging and a fibrin-targeted contrast agent. Circulation. 2005;112:1594–600.
182. Spuentrup E, Botnar RM, Wiethoff AJ, et al. MR imaging of thrombi using EP-2104R, a fibrin-specific contrast agent: initial results in patients. Eur Radiol. 2008;18:1995–2005.
183. Muszbek L, Yee VC, Hevessy Z. Blood coagulation factor XIII: structure and function. Thromb Res. 1999;94:271–305.
184. Jaffer FA, Tung CH, Wykrzykowska JJ, et al. Molecular imaging of factor XIIIa activity in thrombosis using a novel, near-infrared fluorescent contrast agent that covalently links to thrombi. Circulation. 2004;110:170–6.
185. Miserus RJ, Herias MV, Prinzen L, et al. Molecular MRI of early thrombus formation using a bimodal alpha2-antiplasmin-based contrast agent. JACC Cardiovasc Imaging. 2009;2: 987–96.
186. Yun M, Jang S, Cucchiara A, Newberg AB, Alavi A. 18F FDG uptake in the large arteries: a correlation study with the atherogenic risk factors. Semin Nucl Med. 2002;32:70–6.
187. Tatsumi M, Cohade C, Nakamoto Y, Wahl RL. Fluorodeoxyglucose uptake in the aortic wall at PET/CT: possible finding for active atherosclerosis. Radiology. 2003;229:831–7.
188. Ben-Haim S, Kupzov E, Tamir A, Israel O. Evaluation of 18F-FDG uptake and arterial wall calcifications using 18F-FDG PET/CT. J Nucl Med. 2004;45:1816–21.
189. Dunphy MP, Freiman A, Larson SM, Strauss HW. Association of vascular 18F-FDG uptake with vascular calcification. J Nucl Med. 2005;46:1278–84.

190. Rudd JH, Warburton EA, Fryer TD, et al. Imaging atherosclerotic plaque inflammation with [18F]-fluorodeoxyglucose positron emission tomography. Circulation. 2002;105:2708–11.
191. Tawakol A, Migrino RQ, Bashian GG, et al. In vivo 18F-fluorodeoxyglucose positron emission tomography imaging provides a noninvasive measure of carotid plaque inflammation in patients. J Am Coll Cardiol. 2006;48:1818–24.
192. Rudd JH, Myers KS, Bansilal S, et al. (18)Fluorodeoxyglucose positron emission tomography imaging of atherosclerotic plaque inflammation is highly reproducible: implications for atherosclerosis therapy trials. J Am Coll Cardiol. 2007;50:892–6.
193. Tahara N, Kai H, Ishibashi M, et al. Simvastatin attenuates plaque inflammation: evaluation by fluorodeoxyglucose positron emission tomography. J Am Coll Cardiol. 2006;48: 1825–31.
194. Lee SJ, On YK, Lee EJ, Choi JY, Kim BT, Lee KH. Reversal of vascular 18F-FDG uptake with plasma high-density lipoprotein elevation by atherogenic risk reduction. J Nucl Med. 2008;49:1277–82.
195. Wykrzykowska J, Lehman S, Williams G, et al. Imaging of inflamed and vulnerable plaque in coronary arteries with 18F-FDG PET/CT in patients with suppression of myocardial uptake using a low-carbohydrate, high-fat preparation. J Nucl Med. 2009;50:563–8.
196. Rogers IS, Nasir K, Figueroa AL, et al. Feasibility of FDG imaging of the coronary arteries: comparison between acute coronary syndrome and stable angina. JACC Cardiovasc Imaging. 2010;3:388–97.
197. Kwee RM, Teule GJ, van Oostenbrugge RJ, et al. Multimodality imaging of carotid artery plaques: 18F-fluoro-2-deoxyglucose positron emission tomography, computed tomography, and magnetic resonance imaging. Stroke. 2009;40:3718–24.
198. Tahara N, Kai H, Nakaura H, et al. The prevalence of inflammation in carotid atherosclerosis: analysis with fluorodeoxyglucose-positron emission tomography. Eur Heart J. 2007;28: 2243–8.
199. Graebe M, Pedersen SF, Borgwardt L, Hojgaard L, Sillesen H, Kjaer A. Molecular pathology in vulnerable carotid plaques: correlation with [18]-fluorodeoxyglucose positron emission tomography (FDG-PET). Eur J Vasc Endovasc Surg. 2009;37:714–21.
200. Khazen W, M'Bika JP, Tomkiewicz C, et al. Expression of macrophage-selective markers in human and rodent adipocytes. FEBS Lett. 2005;579:5631–4.
201. Rong JX, Shapiro M, Trogan E, Fisher EA. Transdifferentiation of mouse aortic smooth muscle cells to a macrophage-like state after cholesterol loading. Proc Natl Acad Sci U S A. 2003;100:13531–6.
202. Sadeghi MM, Glover DK, Lanza GM, Fayad ZA, Johnson LL. Imaging atherosclerosis and vulnerable plaque. J Nucl Med. 2010;51 Suppl 1:51S–65.
203. Bellin MF, Roy C, Kinkel K, et al. Lymph node metastases: safety and effectiveness of MR imaging with ultrasmall superparamagnetic iron oxide particles – initial clinical experience. Radiology. 1998;207:799–808.
204. Trivedi RA, Mallawarachi C, U-King-Im JM, et al. Identifying inflamed carotid plaques using in vivo USPIO-enhanced MR imaging to label plaque macrophages. Arterioscler Thromb Vasc Biol. 2006;26:1601–6.
205. Tang TY, Howarth SP, Miller SR, et al. The ATHEROMA (atorvastatin therapy: effects on reduction of macrophage activity) study. Evaluation using ultrasmall superparamagnetic iron oxide-enhanced magnetic resonance imaging in carotid disease. J Am Coll Cardiol. 2009;53:2039–50.
206. Fayad ZA, Razzouk L, Briley-Saebo KC, Mani V. Iron oxide magnetic resonance imaging for atherosclerosis therapeutic evaluation: still "rusty?". J Am Coll Cardiol. 2009;53:2051–2.
207. Vymazal J, Spuentrup E, Cardenas-Molina G. Thrombus imaging with fibrin-specific gadolinium-based MR contrast agent EP-2104R: results of a phase II clinical study of feasibility. Invest Radiol. 2009;44:697–704.